THE STRUCTURE OF THE NEMATOCYST THREAD AND THE GEOMETRY OF DISCHARGE IN *CORYNACTIS VIRIDIS* ALLMAN

By R. J. SKAER and L. E. R. PICKEN
Department of Zoology, University of Cambridge

(*Communicated by C. F. A. Pantin, F.R.S.—Received* 23 *February* 1965
—Revised 10 *May* 1965)

[Plates 12 to 21]

CONTENTS

Electron microscope studies reveal that the undischarged nematocyst thread is not (as the light microscope image suggests) a cylinder containing a compact mass of barbs, but a screw, as first shown in the electron micrographs of Bretschneider (1949). In the process of discharge, the screw surface is converted to a cylinder without significant change in surface area. This transformation is markedly anisometric, the length of the thread increasing almost threefold, while the overall increase in diameter is less than 50 %. The screw shape of the undischarged thread is due to the

Vol. 250. B. 764. (Price £1. 8*s*.; U.S. $4.20) 16 [Published 30 December 1965

presence of three helical pleats in the membrane; and discharge results in the smoothing out of these. The cavity of the thread is smaller in the undischarged condition—because of the presence of pleats—and is largely filled by the whorls of asymmetrical barbs (three to a whorl); the tips of the barbs are pressed closely together, while their spatulate bases are distributed in open hexagonal array over the pleated surface of the thread. Barbs readily become detached from the surface of the discharged thread, leaving a complex, striated scar. The discharged thread is a slightly tapering tube in holotrichous isorhizas, and the barbs show systematic changes in size and proportions with taper. Electron micrographs show that the cavity of the undischarged thread is filled with a flocculent material, as is the space between the capsule wall and the thread. This material is presumably the highly hygroscopic proteinaceous working substance responsible for the increase in volume of the capsular fluid—at least up to 200 %—on hydration. The undischarged thread and its contents, isolated under anhydrous conditions, are conspicuously hygroscopic and perform movements of elongation and rotation as water vapour is admitted to or removed from the system. The transformation of a membrane in the form of a screw surface to a cylinder, such as occurs in the discharge of the nematocyst thread, is only possible if portions of the membrane in the trough of the screw increase in area, or portions of the pleats decrease in area. The apparent constancy of the area of the thread throughout discharge suggests that both processes may occur.

Introduction

What seem to have been the first published electron micrographs of nematocysts were those of Bretschneider (1949). These were of 'longitudinal sections through the small nematocysts of the tentacles of a sea anemone, *Corynactis viridis*', cut on a modified early model of the Cambridge rocking microtome. The photographs revealed a new feature in the structure of the nematocyst thread, a feature beyond the limit of resolution of the light microscope. In Bretschneider's words: 'As its chief characteristic, the filament which has a diameter of 500 mμ, shows a torsion which gives it the shape of a deeply cut infinite screw thread'. Ten years later, this same appearance was recorded in micrographs of sections of the nematocysts of *Hydra* (Chapman & Tilney 1959; Slautterback 1961; Chapman 1961) and of *Anemonia* (Mackay 1961, unpublished observations). None of these later observers mentions Bretschneider's paper or makes the comparison with a screw thread, nor do they comment on the possible significance of the implied helical folding of the thread wall; but Hand (1961), and Westfall & Hand (1962), noticing folds in the 'shaft wall' of b-mastigophores of *Metridium*, suggested that these would give added length to the 'tubule' when it discharges.

Bretschneider's suggestive observations were published in a general paper on electron microscopical technique and had not been seen at the time of publication of earlier studies by Picken (1953), and Robson (1953), on nematocysts from this same small, solitary athecate madreporarian, *Corynactis viridis*, the 'Jewel Anemone' (Carlgren 1940) (figure 1). Indeed, Bretschneider's paper was not seen until the present paper was in draft. In the light of the observations of the electron microscopists mentioned above, it had seemed desirable to establish, by means of electron microscopy, whether the wall of the thread in *Corynactis* nematocysts is similarly folded since, notwithstanding the exceptional size of the largest holotrichous isorhizas from this animal, diffraction effects due to the barbs obscure the structure of the wall of the undischarged thread, as seen by bright field, phase and polarized light microscopy.

In three different types of undischarged cnidae of *Corynactis*, electron micrographs have in fact revealed that the thread has the screw-like shape recorded by Bretschneider—the

'small nematocysts' photographed by him were spirocysts. Since the wall of the discharged thread is a smooth, gradually tapering cylinder, the process of discharge must include the unfolding of the screw-like surface of the wall. The object of the observations described here has been to establish how, precisely, the wall of the thread is folded (in the case of the holotrichous isorhizas in particular), and to relate the dimensional changes that occur during discharge to the configuration of the thread in the undischarged condition.

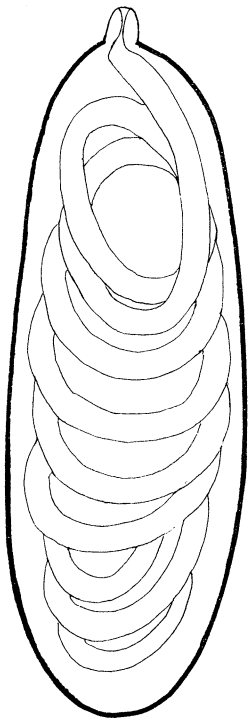

FIGURE 1. Diagram of a large holotrichous nematocyst (approximately 90 μm in length) from *Corynactis viridis*, showing the capsule, the tubular thread, and the region of attachment between thread and capsule. In the light microscope, the wall of the tubular thread cannot be seen. The outline drawn here represents the envelope of the barbs. The barbs themselves are not shown.

2. MATERIALS AND METHODS

The 'anemones' were obtained Mafrom the rine Laboratory, Plymouth, and were successfully maintained for several months in marine aquaria at the Zoological Laboratory, Cambridge. For the preparation of sections of nematocysts, whole animals were transferred from the aquarium at 12 °C to a fluid of the following composition: 2 ml. of an aqueous 5% solution of osmium tetroxide, 0·68 g sucrose and 2 ml. of sea water. This solution was found to preserve the shape of nematocysts more satisfactorily than solutions in which osmium tetroxide was dissolved in M-sucrose solution or in pure sea water. Anemones were placed in the fixative at room temperature, cooled to 3 °C, and left in the fixative for 1 h. They were dehydrated in a graded acetone series at 3 °C, allowed to warm up to room temperature in propylene oxide, and embedded in Araldite epoxy resin (Luft 1961).

In order to obtain sections of the tips of nematocysts arrested in the partially discharged condition, smears were prepared by rubbing a blotted anemone, held in forceps, over a

Polythene sheet. Before the smears dried out, they were placed in a small specimen tube, standing in a bottle containing 2 ml. of a 2% aqueous solution of osmium tetroxide. They were exposed to osmium vapour for 2 h at room temperature and then dehydrated (preceding paragraph) and flat embedded in Araldite. After polymerization of the Araldite, the Polythene was peeled away, leaving the smear embedded in Araldite.

The measurements of barbs and thread (used in constructing the graphs—figures 6 to 9) were made on nematocysts isolated individually from a moist smear with a glass splinter needle, discharged in a drop of distilled water on a grid coated with celloidin, and allowed to dry out in air. Such air-dried specimens were examined in the electron microscope without further preparation.

The perimeters of profiles of undischarged and discharged threads were measured on photographic positive prints with a dial-type map measurer.

3. Observations

(*a*) *The capsule*

Capsules of the holotrichous isorhizas of *Corynactis* vary in size from 13×33 μm to 35×95 μm (Weill 1934). In capsules of average size, the wall is approximately 0·15 μm thick; in those of microbasic mastigophores and spirocysts, on the other hand, it is only about 400 Å thick. In these thinner walled capsules (as Bretschneider first showed), the wall is apparently composed of two sets of clearly defined fibres, oriented parallel and at right-angles to the long axis of the capsule, in a twinned geodetic lattice, and embedded in an electron transparent matrix. The fibres of the two sets are widely spaced in relation to the fibre diameter and are faintly striated. In reality, however, the structure is more complex than Bretschneider supposed. The appearance of an inner set of fibres is due to regular folding of a continuous membrane in folds *ca.* 350 Å thick. Still finer fibrils (*ca.* 40 Å in thickness) run across each fold at a very oblique angle (70 to 80°) (figure 16, plate 12). The outer set of 'fibres' may be what it appears to be; but these fibres are somewhat narrower than the folds of the inner membrane, though also finely striated.

It seems likely that the wall of the larger and thicker walled capsules of the holotrichous isorhizas contains two layers of fibres, inclined at a large angle to each other, but the two sets are not clearly visible. The internal surface of the capsule appears to be smooth. In transverse section, part of the thickness of the wall exhibits striations normal to the tangent to the curve of the wall, and spaced at 99 to 107 Å (figure 17, plate 12). This striation never extends throughout the thickness of the wall in any one section and is most frequently observed in the inner thickness of the wall, adjacent to the capsular fluid. The regions of the wall which lack this fine striation show, however, periodic dark markings, sometimes in the form of parallel dark lines running obliquely across the thickness of the wall with a repeat of 400 to 500 Å (figure 17, crosses). The fine striation already mentioned sometimes displays a discontinuity or discontinuities normal to the plane of striation (figure 17, arrows). This appearance might be accounted for if the striated areas are longitudinal sections of fibrils, running approximately at right-angles to the long axis of the capsule. Such a layer of fibrils, one fibril thick, would show discontinuities if the plane of section were not strictly transverse. No distinct boundary to the fibrils is visible, either

with lead- or uranyl-acetate staining. It is not clear whether the widely spaced dark markings are the fine striations cut obliquely, or the boundaries of a second set of fibrils.

These observations are compatible with the presence of two sets of fibrils, embedded in the substance of the wall and oriented at *ca.* 90° to each other. The presence of two sets of fibrils would not conflict with the observed properties of capsules in polarized light (Picken 1953). The wall of the capsule is isotropic when viewed between crossed Nicols along a normal to the surface, while at the edges it shows a negative spherulitic cross. This characteristic optical behaviour would be reconcilable either with a purely random distribution of fibrillar elements in the plane of the surface, resulting in statistical isotropy, or else with a regular arrangement in which crossed orientation of fibrils results in isotropy by compensation. Conceivably, the layered appearance of the wall, as seen edge-on in polarized light between crossed Nicols, may be related to a real stratification, as suggested by the appearances seen in thin sections under the electron microscope, and not solely to diffraction—as previously suggested.

(*b*) *The region of attachment of thread to capsule*

In the nematocysts of *Corynactis*, no operculum is present, in the sense in which this structure occurs in the stenotele nematocyst of *Hydra*, for example (see Chapman 1961, pp. 139, 145). Nevertheless, the structure of the capsule wall changes—in the spirocysts, for example—in the region of attachment, so that the wall there resembles the wall of the undischarged nematocyst thread (figure 18, plate 13). Much the same structure is to be seen in holotrichous isorhizas. In these capsules, the cavity of the nematocyst thread is largely obliterated in the region of attachment. The thread itself opens out sharply to form the capsule wall of the attachment region.

(*c*) *The undischarged thread*

The thread of the undischarged nematocyst is a tube, the wall of which is helically folded, much as a tube of paper becomes folded if twisted while under tension. In the interests of clarity, the region where the surface is folded will be referred to as 'a fold', while the two thicknesses of the surface brought together by folding will be referred to as 'a pleat'. Three pleats run round the thread in left-handed helices, the pitch angle of which varies from 28 to 44°. In order to measure this angle, the edges of the helices on one side of a print of a median section of the thread were joined by a straight line (line 1) (figure 19, plate 14). A perpendicular (that is, the maximum diameter of the undischarged thread) was dropped from this line across the print, and starting from a convenient edge on the opposite side of the thread, a second straight line, parallel to the first, was drawn (line 2). Since there are three helices, if we start counting sectioned helical edges from any given section, the fourth edge will be part of the helix from which we started. The distance between the first and fourth helical edges along line 1 is, by one definition, the 'pitch' of the helix. But since there are three helices, we propose to define the steepness of the helix by reference to the pitch angle, in order to avoid ambiguity. If oblique straight lines are drawn, from a point midway between the first and fourth helical edges on line 2, to the intercepts between the first and fourth edges and line 1, the angle between the oblique lines and the diameter of the thread is the pitch angle of the helix. It

must be emphasized that this angle is measured between straight lines, on a median plane, rather than between the tangent to the helix and the circumference, at the surface. Measurements of this angle were made both on partially discharged and undischarged threads.

The pitch angle varies systematically along the thread, increasing as the diameter of the thread decreases.

The plane of each pleat at its origin, as seen in strictly transverse section, is normal to the surface of the core (see below) of the undischarged thread (figure 20, plate 14), but the greater part of each pleat is itself folded in a clockwise direction (looking from the advancing tip—the *dart*—down the axis of the thread). As seen in transverse section, the profile of a pleat is a sigmoid curve, occupying about one-third of the periphery of the thread. More accurately described, immediately after the 'elbow' where it arises, the surface of the pleat curves successively inwards, outwards and inwards again towards the axis of the thread. This inward curving of the pleat appears in lateral view as an elongate depression. The depressions in successive pleats are in register, so that the cylinder of the thread is to this extent fluted. The *core* of the thread is formed by the central mass of barbs, surrounded by closely adherent regions of the wall. The folding of the wall is made yet more complex by the fact that the barb bases are inserted at the bottom of pockets in it. These are longer as seen in transverse section than in longitudinal section, and in transverse section they arise at a point a short distance along one helical pleat (figure 20, arrow) and extend to the point of origin of the next (different) helical pleat.

The wall of the thread itself is complex in structure. In transverse sections of threads in capsules fixed in osmic sucrose/sea water, the profiles of the wall are 160 Å thick, finely striated, and bordered on each side by a dark line (figure 21, plate 15). The surface in contact with the capsular fluid is covered with a layer of granules, approximately 80 Å in diameter, in open array. In threads in capsules fixed in osmium vapour, however, the wall is 290 Å thick and covered with an outer granular layer, 64 Å thick. The technique of preparation clearly influences greatly the apparent dimensions and texture of the wall. It seems likely that the thickness of the wall decreases as the diameter of the thread decreases.

In the undischarged thread of holotrichous isorhizas, the barbs are arranged in alternating whorls of three barbs, as in the hexagonal array shown in figure 2*a*, taken from Picken (1953). The proximal third of a barb will be referred to as the barb base. The barb bases are in reality neither close packed nor circular—as they appear to be (since their dimensions are near the limit of resolution) in the light microscope—but broad, approximately triangular, curved plates. The tips of the barbs are closely packed and overlap each other in a counter-clockwise direction (looking from the tips of the barbs towards their bases), but the shafts and barb bases are not close packed (as in the light microscope image). Each transverse section of the thread of large holotrichous isorhizas includes twelve to fifteen barbs, sectioned at various levels (figure 20), and regularly arranged in a pattern of triadic symmetry. This pattern may be interpreted as a transverse section of three helical rows of barbs, to be referred to henceforth as the *barb helices*. (Inspection of the discharged thread shows, as we shall see, that this interpretation is valid.) Thus accurately transverse sections include portions of five barbs from each of the three barb helices.

The shortest distance between successive whorls of barb bases in the undischarged state will be referred to as the *whorl separation.*

Notwithstanding the large differences in diameter between different parts of the thread, due to taper, and in spite of gross variation in the sizes of capsules—with associated differences in thread diameter, the whorl separation is fairly constant at a value varying between 0·4 and 0·5 μm. This constancy is correlated with increase in the pitch angle of the helical pleats with taper (figure 3). The decrease in the number of cross-sectioned

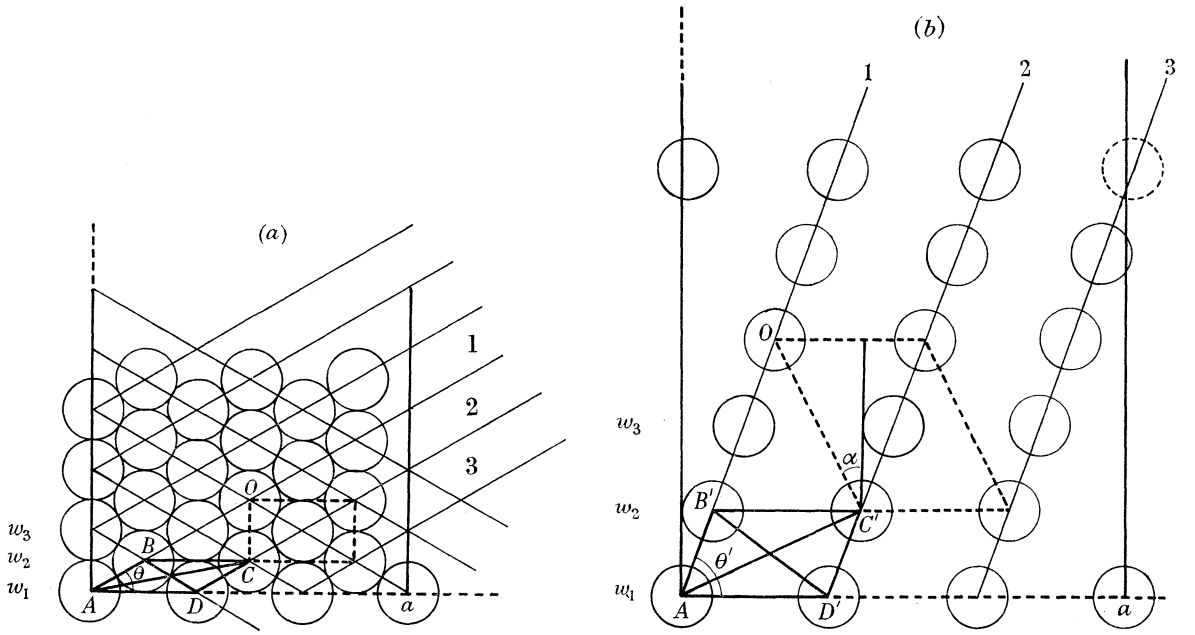

FIGURE 2. (*a*) Diagram showing the disposition of the barb bases in close hexagonal array on the surface of the undischarged thread regarded as a plane sheet, as seen in the light microscope. w_1, w_2 and w_3 are three successive whorls of three barbs; 1, 2 and 3 are three helical barb rows, each of inclination θ; lines of opposite inclination unite barb bases belonging to different barb rows. *A* and *a* are the same barb base. *ABCD* is a unit cell of the pattern of barb bases. In the figure, barb *O* is equidistant from *A* and *a*, and the dotted line *OC*, parallel to the axis of the undischarged thread, joins barbs of alternate whorls. The rectangle of which *OC* is one side is transformed to a parallelogram on discharge (figure 2*b*). In order to facilitate comparison with the pattern of barb bases after discharge (figure 2*b*), figure 2*a* is drawn as if rotated through 180° about the axis *Aa*. This rotation is in effect what happens when the discharging thread everts.

(*b*) After discharge (including eversion), the barbs are still evenly spaced round the circumference in whorls of three, and there are three helical barb rows, 1, 2 and 3. The inclination of these has changed from θ to θ', and the parallelogram *ABCD* has transformed to *AB′C′D′*. The previously vertical line, *OC*, has rotated through an angle α. The significance of α is discussed in §5, and in the Appendix.

barbs from 15 to 12, near the tip of the thread, is also due to this approximate constancy of whorl separation. The length of the barbs decreases with decrease in the diameter of the thread (p. 143), so that (with the whorl separation remaining virtually unchanged) barbs at the tip of the thread overlap each other less than do those at the base of the thread.

The barbs are asymmetrical and, their structure is best seen in discharged threads (p. 139). Each consists of an approximately planar, triangular *base*, the base line of which is not straight but slightly curved (figure 22*a*, plate 15). The base converges into a *shaft*, elliptical in transverse section (figure 23, plate 16), and garnished towards the tip with two (rarely three) *barbules* (figure 22*b*, plate 15) that lie in a radial plane, in relation to the entire thread, and are presented towards the inner surface of the thread wall in the undischarged condition (figure 19, plate 14). In a high proportion of cases, the shaft is seen to be

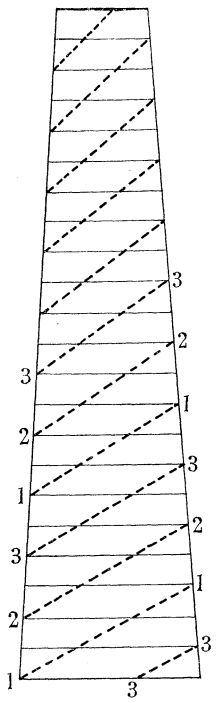

FIGURE 3. Schematic diagram showing how with constant whorl separation the pitch angle of three helical lines around a tapering tube must increase as the diameter diminishes. The three helices are numbered 1, 2 and 3. This diagram is in no way a representation of the nematocyst thread.

slightly curved, with the concavity directed towards the inner surface of the thread wall. The tangent to the mid-point of the curve of the shaft makes an angle of about 25° with the long axis of the thread. The projection of the barb on the plane at right-angles to its plane of curvature does not coincide with the long axis of the thread, however, but is slightly tilted, so that the distal end of the barb overlaps one of its neighbours in its whorl, and is itself overlapped by the remaining member of the trio. This overlap is shown in transverse sections of the dart in threads arrested in discharge (figure 23, plate 16).

In microbasic mastigophores, the thread is more obviously a screw, as seen in longitudinal section, than it is in holotrichous isorhizas. The barbs of the 'filament' (Hand's term for the narrow region of the thread) are more strongly curved than in the holotrichous isorhizas, so that they resemble plant thorns (figure 24, plate 17), while the barbs of the shaft or butt are elongate spatulae (Robson 1953, figure 2*E*). In spirocysts, the thread is totally devoid of barbs (in contrast to the figures for spirocysts of *Corynactis* given by Cutress (1955)). The undischarged thread (figure 16, plate 12) contains irregular masses of

FIGURE 16. Tangential section of spirocyst capsule showing striated, outer fibres (*o.f.*); folds, *ca.* 350 Å thick (*fo.*), and finer fibrils (*ca.* 40 Å) (*f.f.*); longitudinal sections of the thread (*th.*); lightly and darkly stained thread contents, tabular crystal-like aggregates (*tab.*) and pleats (*pl.*).

FIGURE 17. Cross-section of capsule of a holotrichous isorhiza showing fine striation. Arrows mark discontinuities; crosses mark oblique, darker lines. Capsular fluid (*c.f.*); cnidoblast cytoplasm (*cyt.*).

(*Facing p.* 138)

FIGURE 18. Longitudinal section of the distal end of a spirocyst showing change in structure of the capsule around the region of attachment (*a.*) of the thread (*th.*). Plasma membrane of cnidoblast (*p.c.*); plasma membrane of flagellated ectodermal cell (*p.f.*). The segments of cytoplasmic fibrils at × are characteristic of the cytoplasm covering the distal end of this type of capsule.

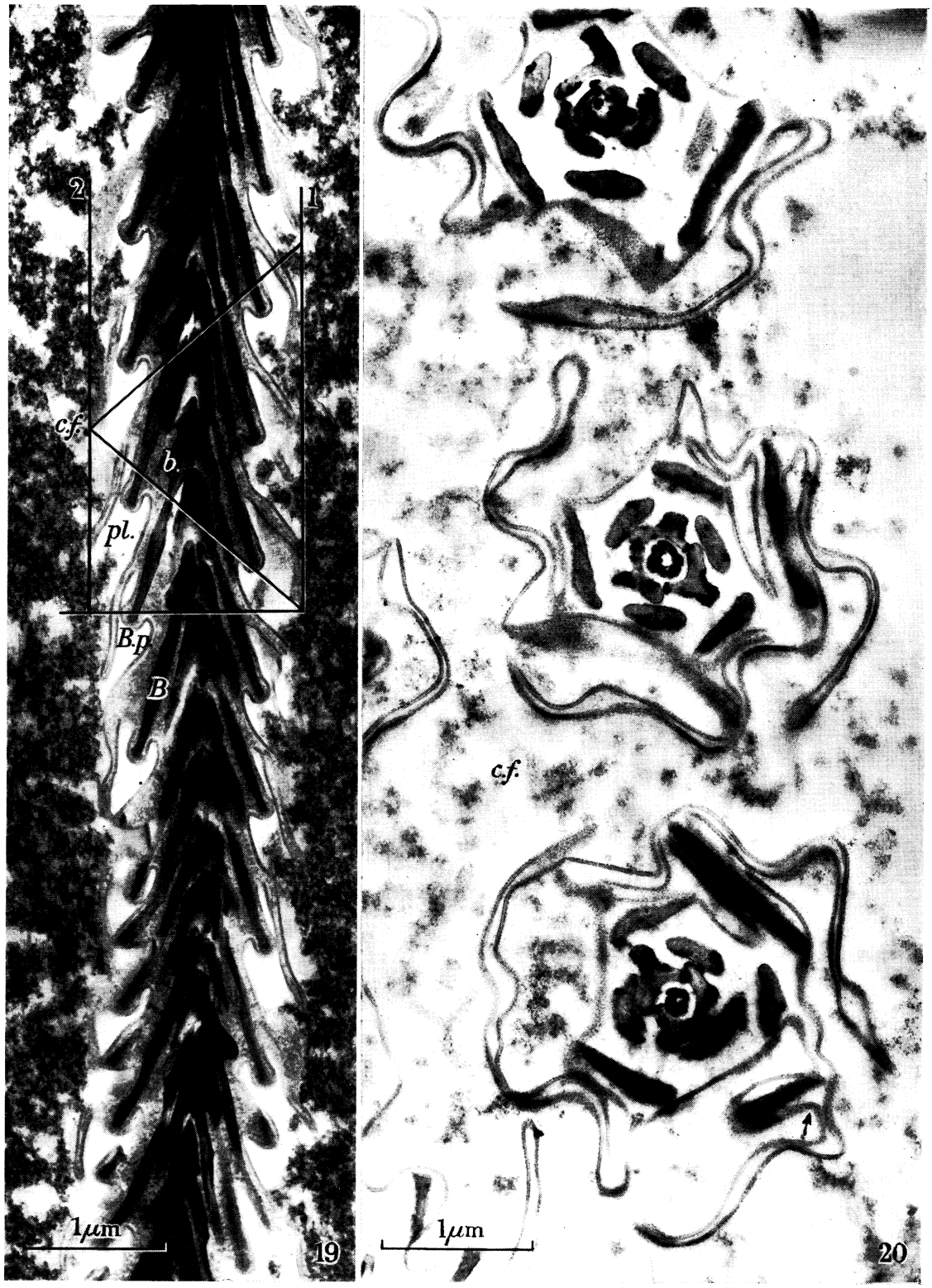

FIGURE 19. Median longitudinal section of the undischarged thread of a small holotrichous isorhiza, fixed in the capsular fluid (*c.f.*). (See text, p. 135.) Barb (*B.*), barb-pocket (*B.p.*), barbule (*b.*), pleats (*pl.*).

FIGURE 20. Transverse sections of the undischarged thread of a large holotrichous isorhiza fixed in the capsular fluid (*c.f.*).

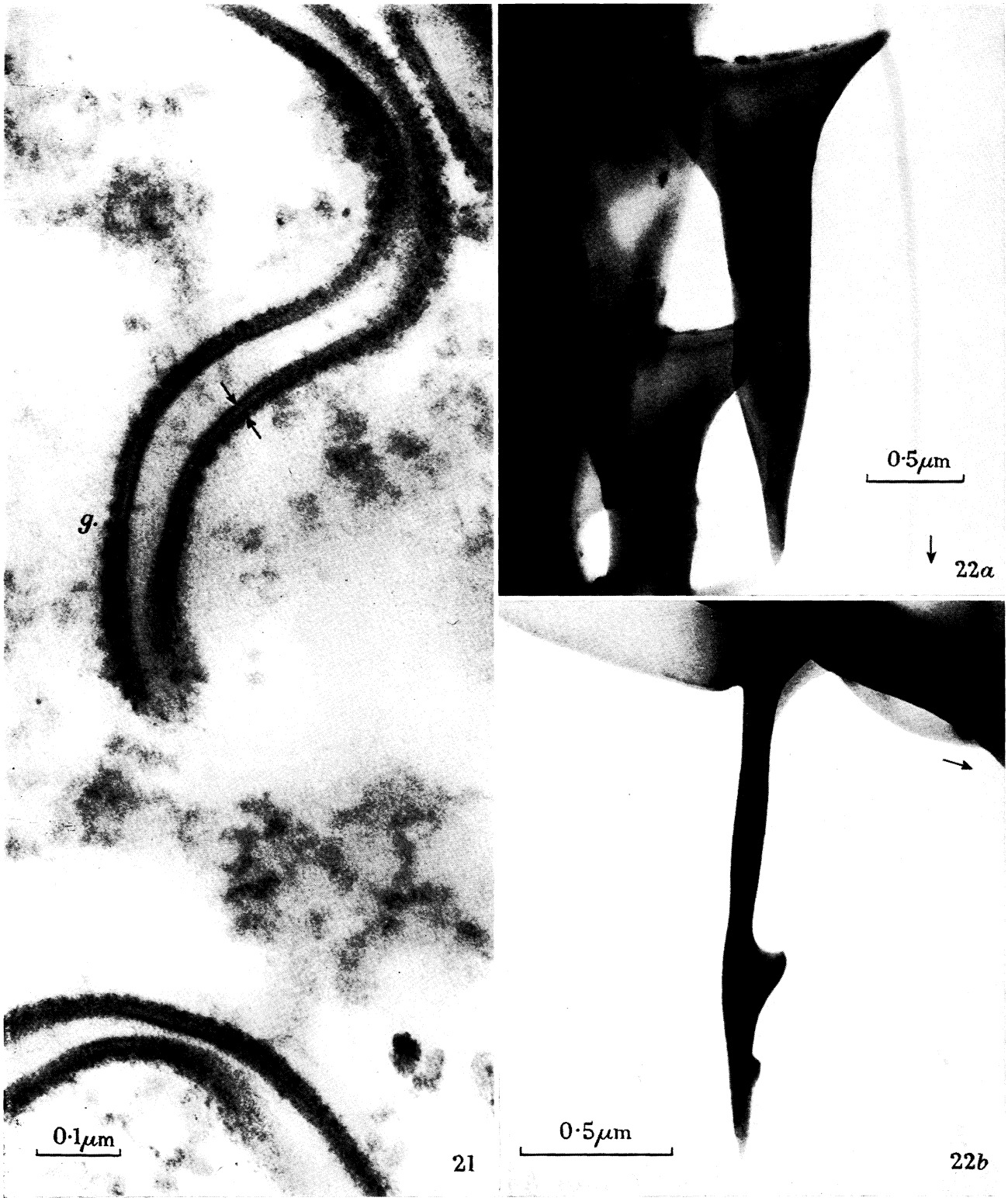

FIGURE 21. Transverse section of the wall of the undischarged thread of a large holotrichous isorhiza fixed in osmic-sucrose/sea water. The profiles of the wall are 160 Å thick (between arrows), finely striated, and bordered on each side by a dark line, in places apparently resolved into a row of granules. The surface in contact with the capsular fluid is covered by a layer of granules (*g.*), approximately 80 Å in diameter, in open array.

FIGURE 22. Single barbs on the discharged thread of a large holotrichous isorhiza, dried in air; (*a*) in plan; (*b*) in side view. The arrows point towards the capsule.

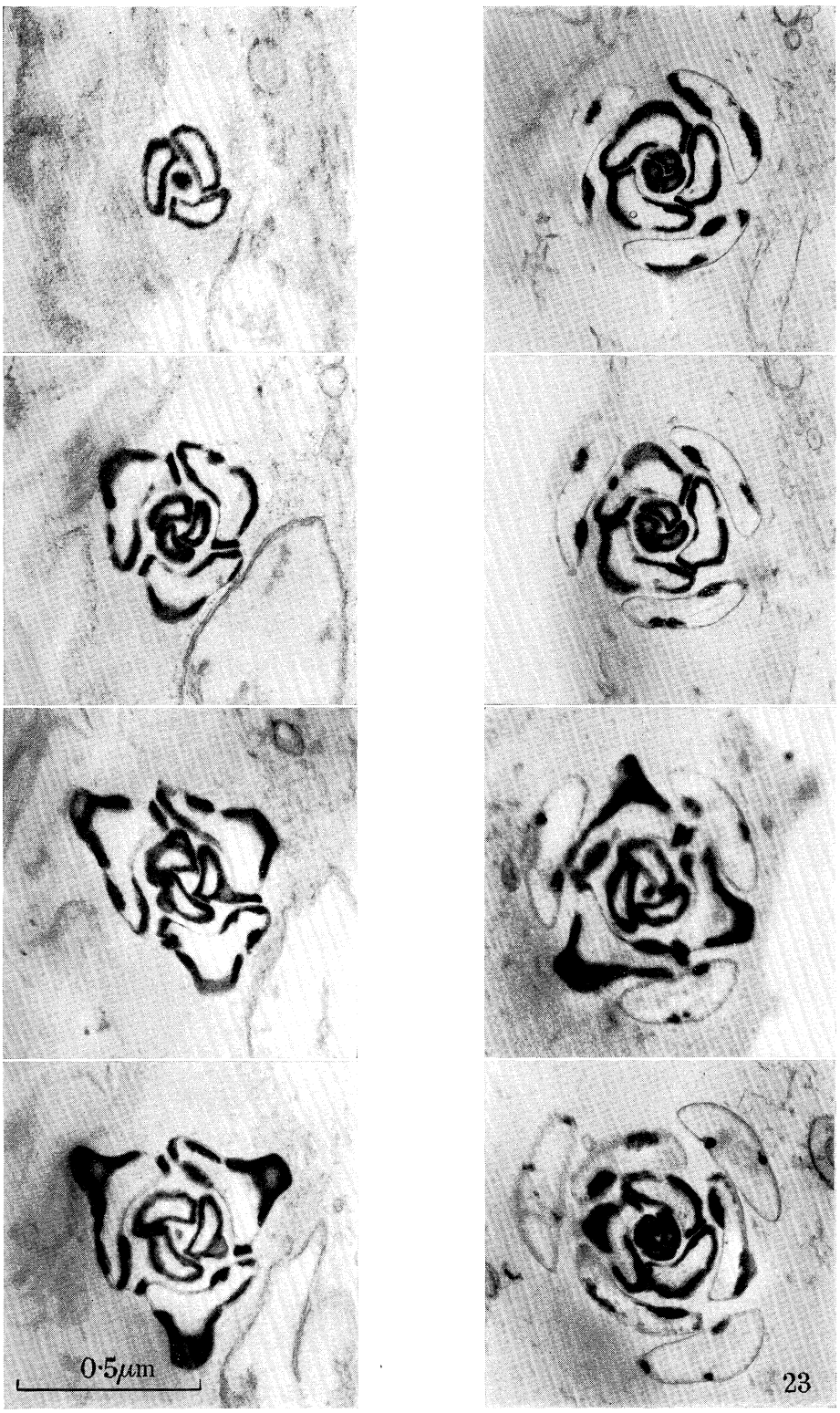

FIGURE 23. Accurately transverse serial sections of a dart from a thread arrested in discharge in a smear from a tentacle, showing the overlap between barbs of the same whorl, and the high electron-density of the barbules and of asymmetrically placed regions of the shaft.

FIGURE 24. Longitudinal section of an undischarged capsule of a microbasic mastigophore. The barbs (*B.*) (see text, p. 138) are strongly curved and without barbules.

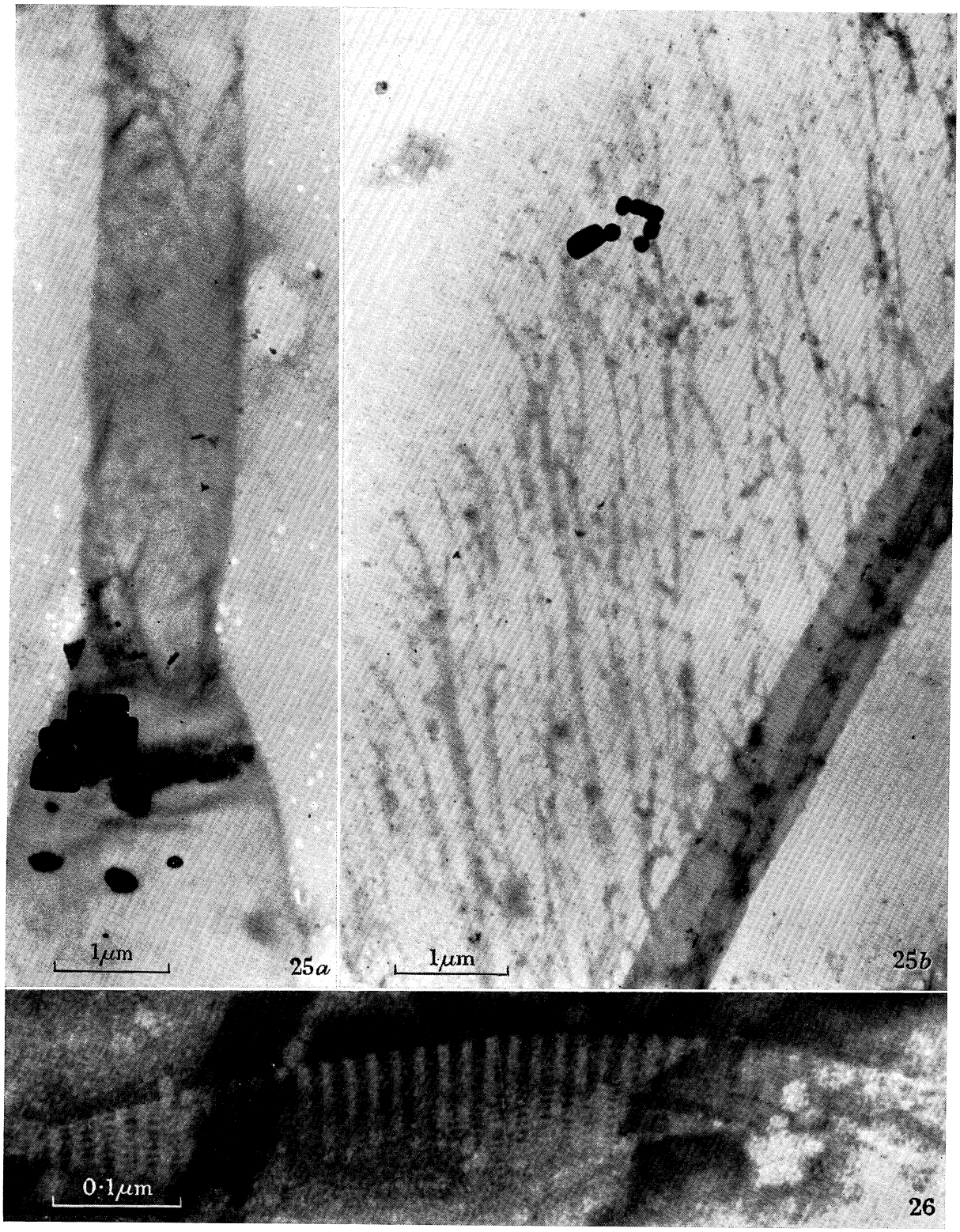

FIGURE 25. (*a*) Discharged spirocyst-capsule (air dried) showing faint helical markings of steep inclination on the lower part of the discharged thread. (*b*) The *Flimmer*-like anastomizing strands of material on one side of the discharged thread. The 'core' of the thread is probably a fold in the thin tubular wall, and the dense particles may be sodium chloride.

FIGURE 26. Scar marking the attachment of a barb to the surface of the discharged thread of a large holotrichous isorhiza, air-dried and negatively stained with potassium phosphotungstate.

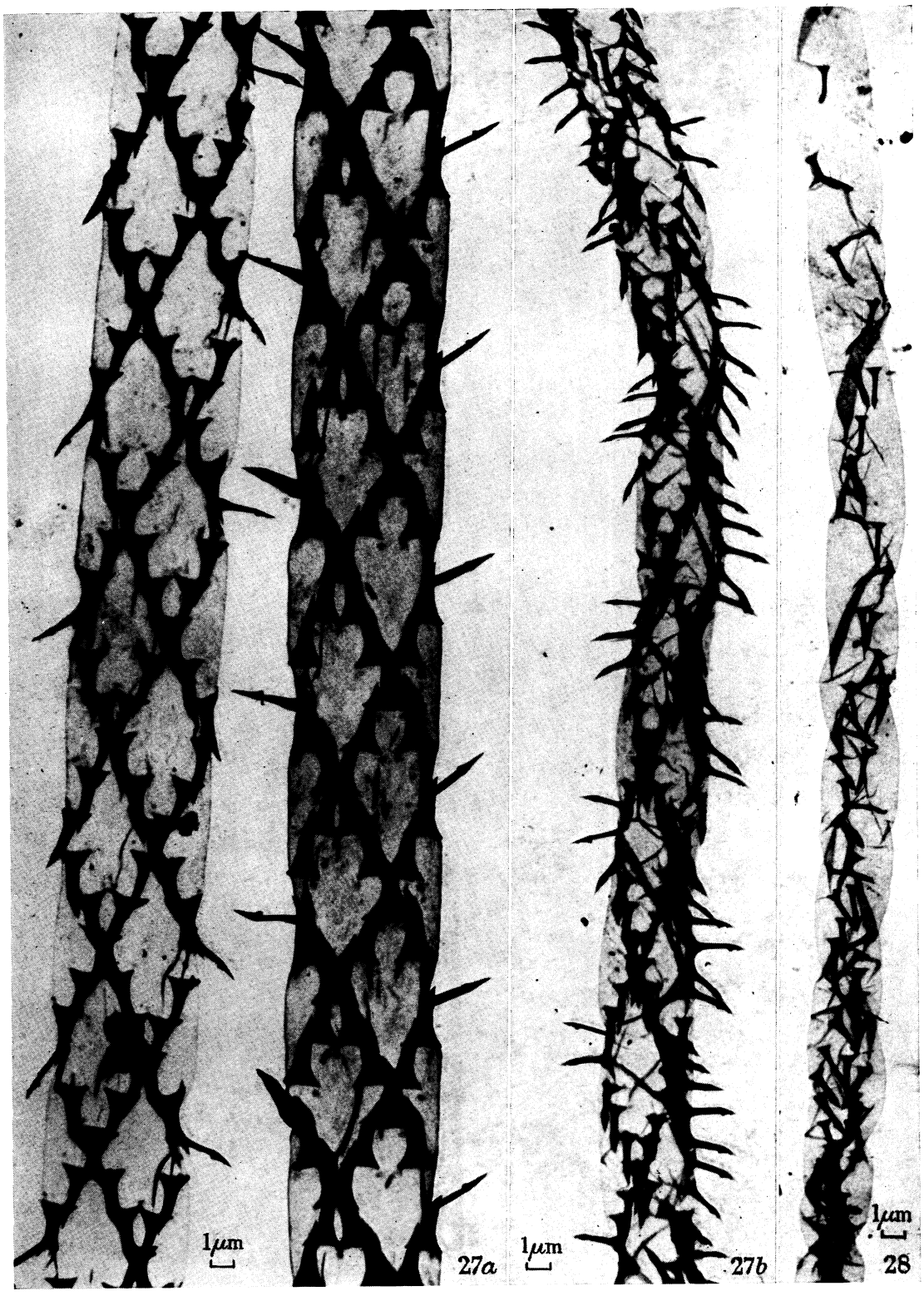

FIGURE 27. Air-dried discharged threads from two holotrichous isorhizas (*a* and *b*), flattened to differing extents, showing barb-whorls and the staggering of the whorls, so as to form three rows of barbs.

FIGURE 28. Air-dried thread discharged without eversion by bursting the capsule of a holotrichous isorhiza in distilled water. The most anterior barb, without near neighbours, is as asymmetrical as those in triads. The tip of the thread is just off the top of the photograph.

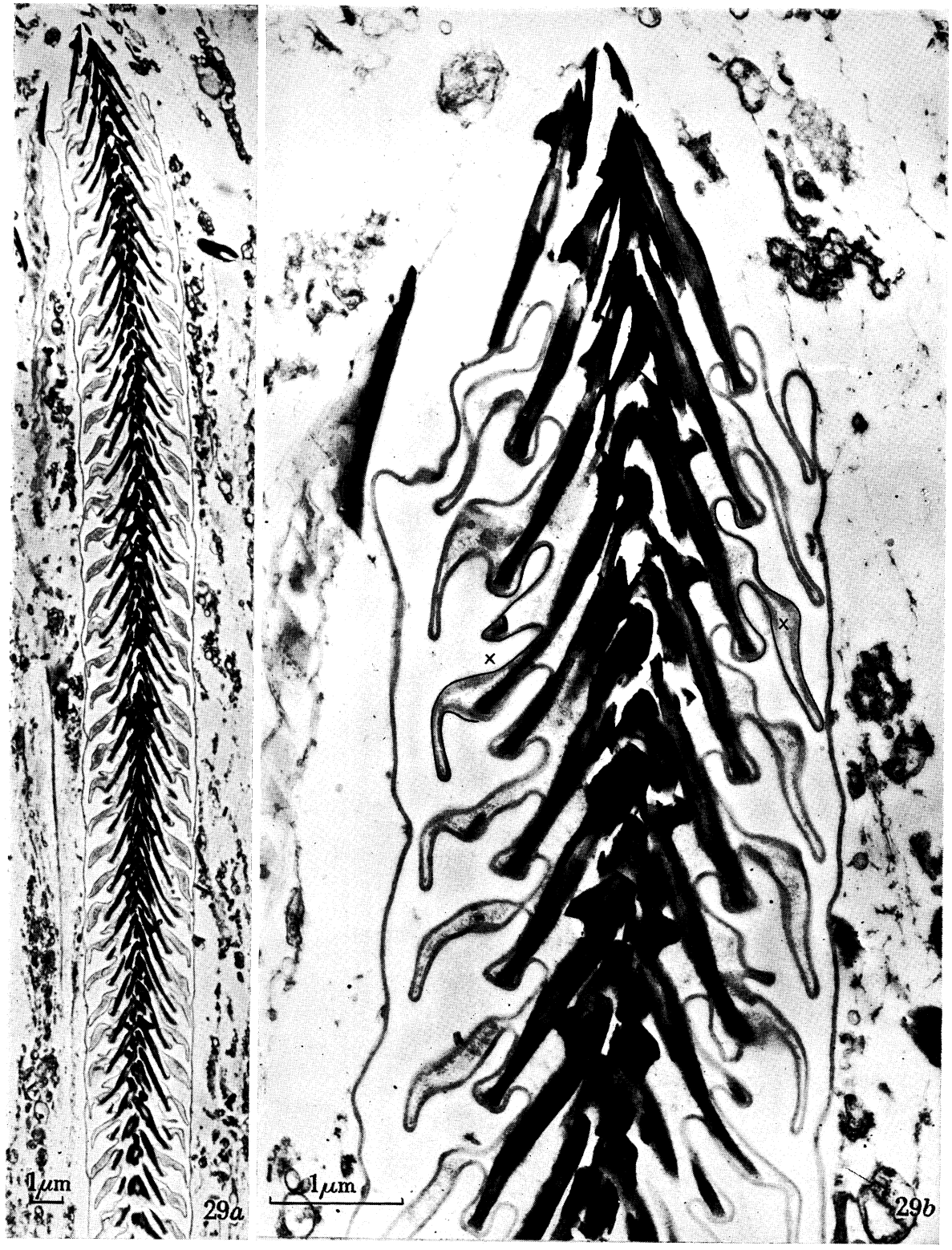

FIGURE 29. (*a*) Accurately median longitudinal section of dart and thread of a large holotrichous isorhiza arrested in discharge in a tentacular smear. (*b*) The dart and tip of this same section under higher power. The barbs have fallen from the discharged surface. In *b* the inked-in right- and left-hand profiles are those used to determine the area of the internode (p. 149). In each case the cross marks the centroid of the curve.

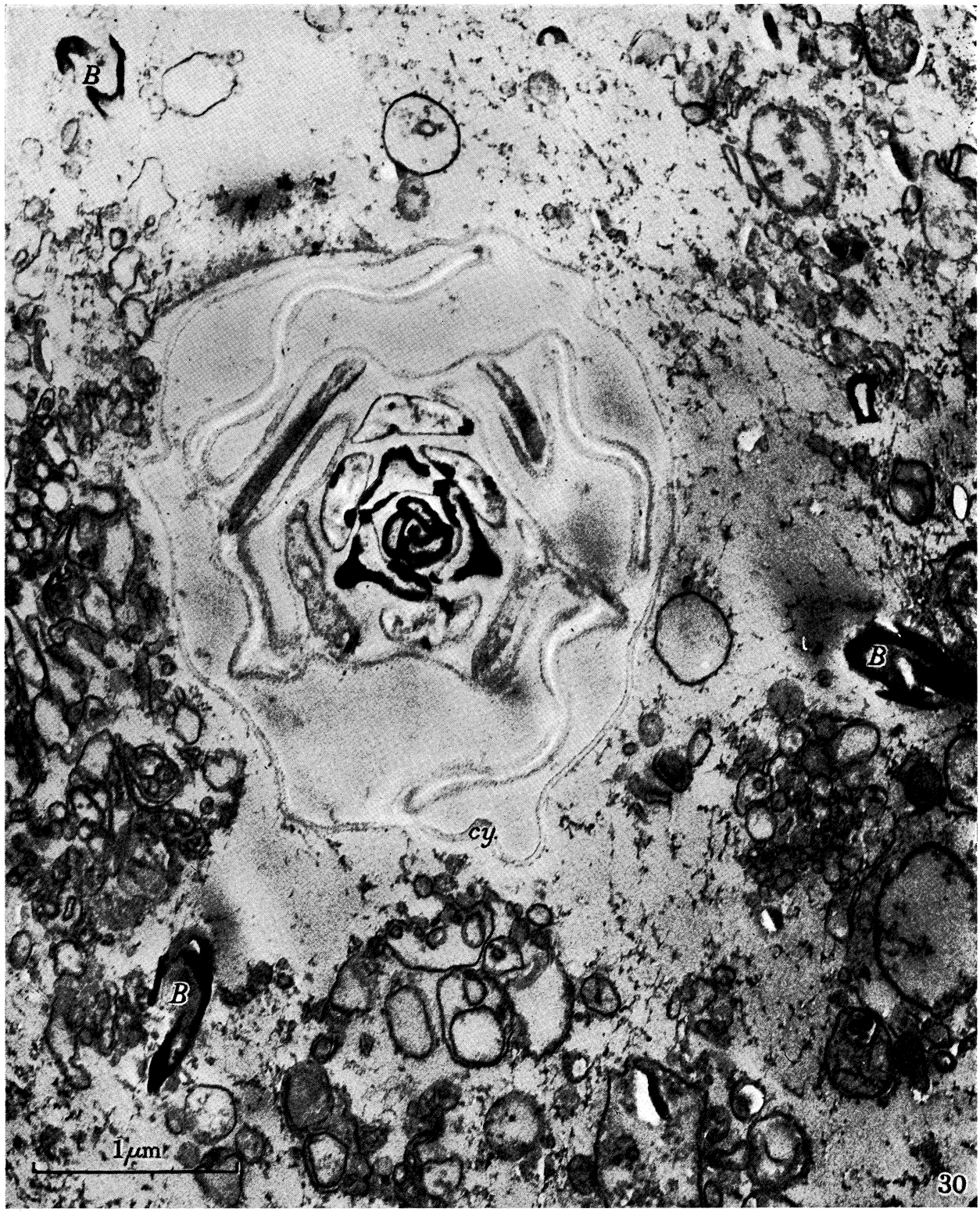

FIGURE 30. Accurately transverse section of an arrested tip, showing portions of one whorl of barbs (*B.*) from the outer surface of the discharged cylinder itself (*cy.*) and th eundischarged thread (as in figure 20, plate 14) within.

densely staining material of two kinds—more darkly and more lightly staining—as well as tabular, crystal-like aggregates. After discharge, the spirocyst thread is electron transparent and exhibits faint helical markings of steep inclination (figure 25*a*, plate 18). In smears made directly on carbon-coated, celloidin-covered grids, by touching the grid against a tentacle and stimulating with an electrical stimulus, the discharged spirocyst thread carries a *Flimmer* of irregularly anastomosing strands of material of low electron density, usually distributed on one side only of the thread, in a manner recalling the appendages of certain flagella of phytoflagellates (figure 25*b*, plate 18). This appearance is presumably produced by traction during preparation.

(*d*) *The capsular fluid*

In Araldite sections, the capsular fluid appears as a coarse, granular flocculum (figures 19, 20, plate 14). Indeed, some capsules—provisionally regarded as immature—have very darkly staining contents. The space within the nematocyst-thread usually contains more finely granular, and less darkly staining, material than the capsular fluid itself.

(*e*) *The discharged thread*

The discharged thread of a large holotrichous isorhiza is a tube that tapers gradually from a diameter of 5 μm at its base to 2 μm at its tip. Cutress (1955) suggested that large nematocysts found in the Corallimorpharia (including *Corynactis*), and hitherto described as 'holotrichs' are in fact macrobasic p-mastigophores, with a shaft more than three times the length of the capsule, abruptly reduced to a thread that may be more than two-thirds the diameter of the shaft. Our observations on the large nematocysts of *Corynactis* have never confirmed such an abrupt reduction in diameter of the thread. On the other hand, the thread is never 'isodiametric' (in the sense of being of constant diameter) as described by Weill (1930) and re-affirmed by Hand (1961).

In electron micrographs, the thickness and structure of the wall of the discharged thread correspond exactly to those of the undischarged thread, provided that both have been fixed, dehydrated and embedded in the same way. Negatively stained, discharged threads occasionally show a faint corduroy-weave pattern, parallel to the long axis; but neither wet nor dry threads tear along a preferred direction. The hint of some degree of orientation of the wall substance parallel to the long axis of the thread, given by the electron micrographs, might be correlated with the observed weak, positive birefringence of the discharged, wet thread, with respect to its length (Picken 1953, pp. 206, 207). The wet thread is reversibly extensible and can be stretched to (roughly) twice its resting length. During discharge, barbs are occasionally detached from the wall. Electron micrographs show that the insertion of a barb is marked by a scar with a doubly banded structure: a coarse banding (periodicity 190 Å) lies at right-angles to the long axis of the thread, and a finer banding (periodicity 50 Å) lies at right-angles to this (figure 26, plate 18). In longitudinal section, the inner and outer faces of the barb appear to be attached to the wall by two junctions (figure 4). Above the region of insertion, the barb itself narrows somewhat.

As in the undischarged thread, the barbs are evenly spaced round the circumference in

whorls of three (figures 2*b*; and 27*a*, plate 19). In the holotrichous isorhizas, the whorls are transverse to the long axis of the thread. Each whorl is slightly staggered to the right of the one below it, so that the thread is armed with three counter-clockwise, helical rows of barbs (figure 27). The angle (p') between a row and a whorl, measured with the thread completely flattened is 65°, and this angle is less than the pitch angle (p'') as defined on p. 135, measured on a median longitudinal section of the unflattened discharged thread, since half the circumference of a tube is always greater than the diameter. It can be shown that

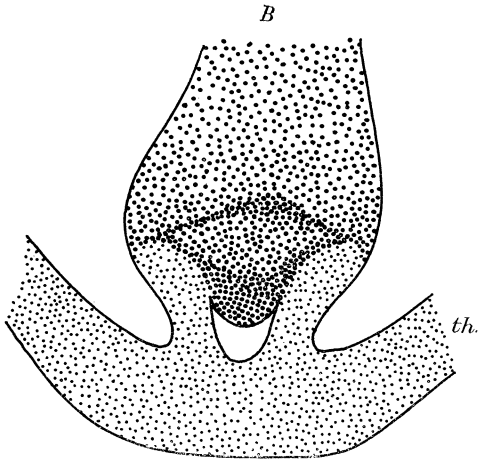

FIGURE 4. Drawing of the insertion of a barb (*B*) on the wall of the undischarged thread (*th.*) as seen in a longitudinal section, strictly at right-angles to the plane of the barb base. No interpretation of the differences in density shown in the diagram can be offered as yet.

$\tan p' = (2\tan p'')/\pi$. If the slope of the barb rows, measured on the completely flattened discharged thread is 65°, the corresponding pitch angle of the barb rows on the cylindrical thread will be about 73°.

The staggering of the whorls is less than the length of the line of attachment of the barb base, so that a longitudinal section of the thread could pass through two adjacent barb bases in the same helical row of barbs.

The barbs themselves (as already stated) are structures without a plane of symmetry. The two barbules (figure 22*b*, plate 15) lie on the side of the barb directed away from the dart; and they, and the tip of the barb, have a high electron density in sections stained with lead- or uranyl-acetate (figure 23, plate 16). In transverse sections, and below the level of the barbules, the barb shaft exhibits two (and occasionally more) asymmetrically placed regions of dense staining. Barbs are absent from the tip of the nematocyst thread, and near the tip their distribution is irregular. Even when the most anterior barb occurs in isolated position, without near neighbours, it is still an asymmetrical structure. This is particularly well shown in threads discharged without eversion, obtained by bursting the capsule in distilled water (figure 28, plate 19).

A study of the dimensions of the barbs of entire, discharged threads was undertaken in order to determine whether there are systematic changes in the barbs, correlated with the taper of the thread. These observations were made on threads dried in air on coated grids. The series of photographs shown in figures 27*a*, *b*, plate 19, suggests that it is possible to

distinguish by inspection threads that have been completely flattened by drying from those that are partially flattened. By selecting photographs of fully flattened threads and measuring the width of the thread, it is therefore possible to determine the circumference of the thread at various levels.

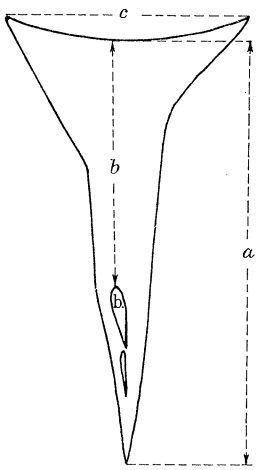

FIGURE 5. Diagram to show how the lengths *a*, *b* and *c*, used in the construction of figures 6 to 9 are defined. As drawn, the barbules (b.) point downwards into the plane of the page—that is, they are on the underside of the barb. Note the asymmetry of the barb, also shown in figure 22, plate 15.

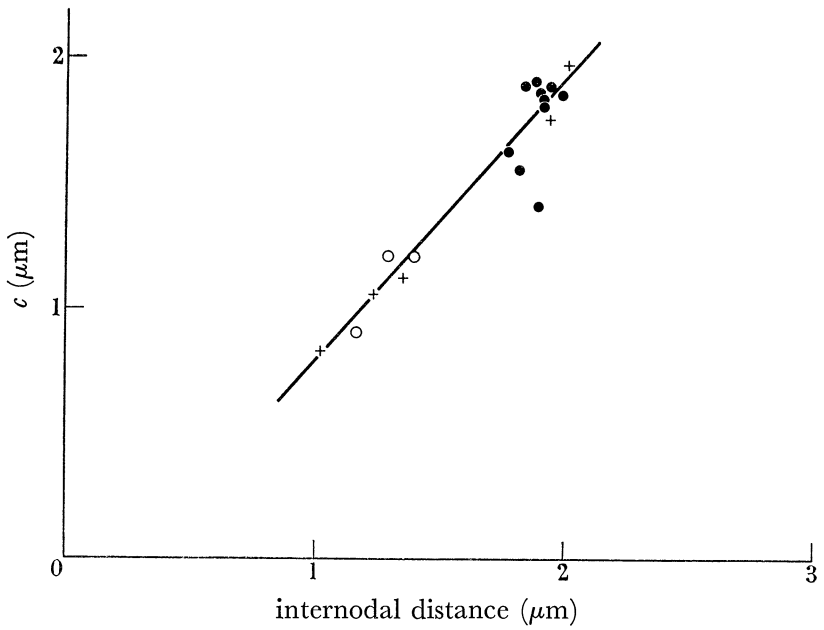

FIGURE 6. Graph relating *c* (maximum width of the barb, figure 5) to internodal distance. Each point is the average of measurements on up to ten different barbs and ten different measurements of internodal distance within a 'convenient' length (see text, p. 143). Data obtained from air-dried, discharged threads. Capsules of holotrichous isorhizas: ●, large; +, medium; ○, small.

The particular dimensions of the barbs chosen for measurement were: the shortest distance from base to tip: *a*; the shortest distance from the base to the crest of the larger barbule: *b*; the maximum width of the barb: *c* (figure 5). While the ratios of the mean values of *a*, *b* and *c*, namely *c*/*a* and *c*/*b*, vary systematically along the thread (figures 8, 9),

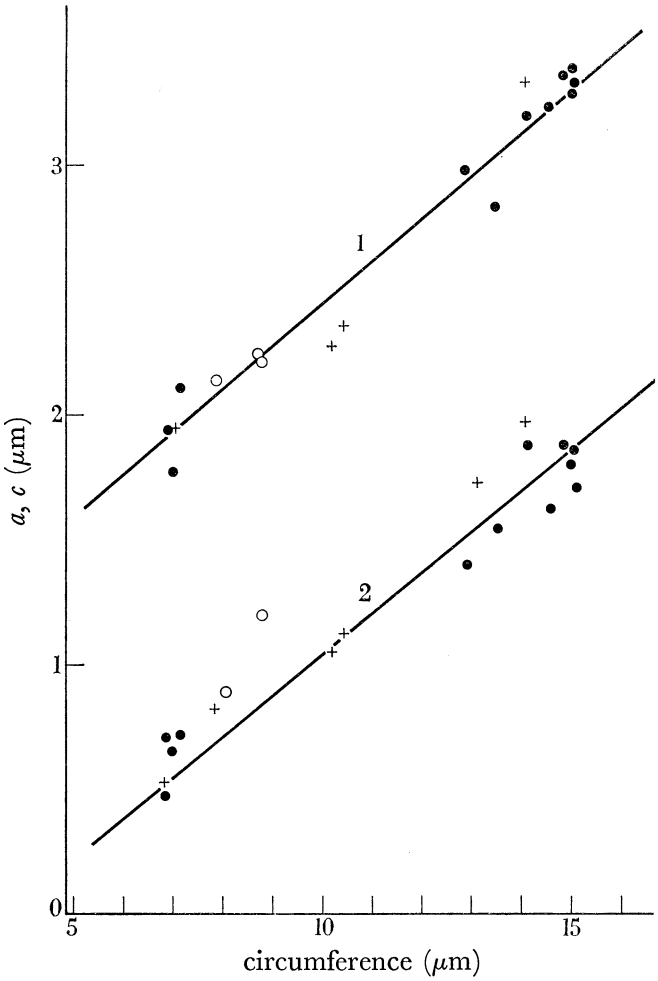

FIGURE 7. Graphs relating (1) *a* (shortest length from the base of a barb to its tip, figure 5), and (2) *c*, to the circumference of the discharged thread. Prepared in the same way as figure 6. Key as in figure 6.

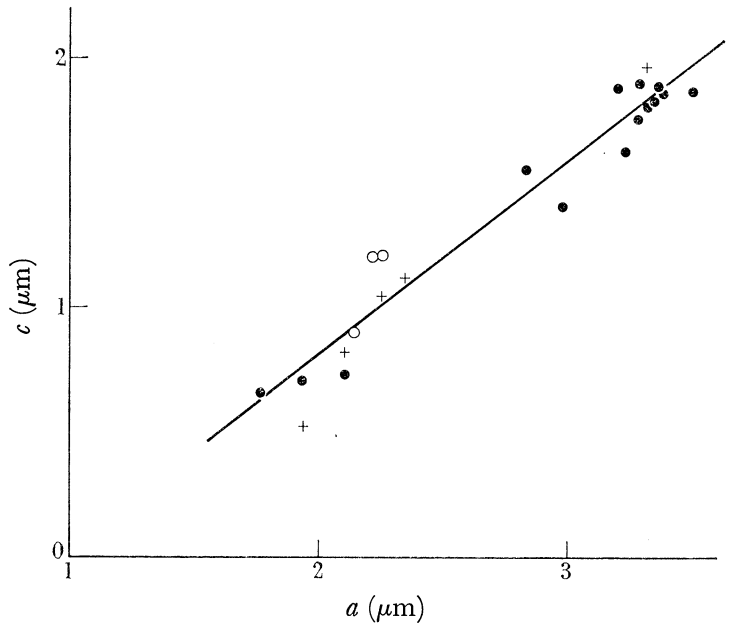

FIGURE 8. Graph relating *c* to *a*. Prepared in the same way as figure 6. Key as in figure 6.

so that the mean dimensions of the barbs over a convenient length are correlated with the circumference of the thread in the same region (figure 7), the ratios themselves are not constant for single barbs in any region. (A 'convenient' length of the thread is one sufficiently long to yield a satisfactory sample of barbs, and yet not too long for all barbs within the length to be observed simultaneously.) There is no correlation between deviations from the mean values of the lengths *a*, *b* and *c*, in barbs that are near neighbours; and in a given region, the dimensions of individual barbs may vary by as much as $\pm 7{\cdot}5\%$. There exists however, a general correlation between the mean dimensions of the barbs in any one region of the thread and the circumference of the thread in the same region.

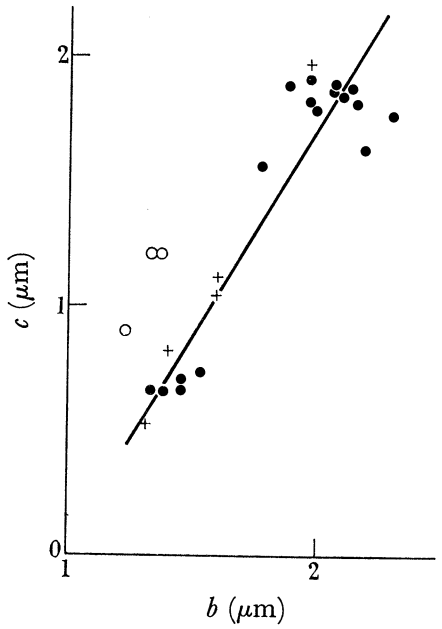

FIGURE 9. Graph relating *c* to *b* (shortest length from the base of a barb to the crest of the larger barbule, figure 5). Prepared in the same way as figure 6. Key as in figure 6.

Figures 6 to 9 distinguish between points derived from measurements on small, medium-sized and large holotrichous isorhizas respectively. It is evident that such points belong to the same straight line. This means that the tips of the threads from large holotrichous capsules closely resemble in their proportions the bases of the threads from small capsules of the same type.

4. COMPARISONS OF UNEVERTED AND EVERTED THREADS

The area of the wall of the thread between successive whorls of barbs will be referred to as an *internode* of the thread. In the undischarged state, this unit is complexly folded, while in the discharged state it is smoothed out and may be regarded, for all practical purposes, as a cylinder. In the absence of a method for directly comparing the dimensions of the entire uneverted thread with those of the entire everted thread, so as to determine what dimensional changes, if any, occur during discharge, it has been necessary to compare the area of an internode before discharge with that of an equivalent internode after discharge. Since the intact, folded internode is electron opaque in the undischarged state, it can be

studied only by means of sections, whereas the dimensions of an equivalent, intact internode in the discharged state can be determined (theoretically, at least) from graphs constructed from measurements on air-dried material. It is necessary first to check, however, whether measurements on air-dried material differ from those on material embedded in Araldite. Preliminary observations on the influence of the method of preparation on the thickness of the thread wall (p. 136) had already suggested that the method of processing markedly alters the dimensions of some parts at least of the thread.

(*a*) *Comparison between the dimensions of Araldite-embedded material and the dimensions of air-dried material*

A comparison was made between the dimensions measured on a median longitudinal section of a discharged thread (figures 29*a*, *b*, plate 20) and the dimensions of apparently comparable parts of the thread obtained from figures 6 to 9. It was assumed that the distance from barb base to barbule would vary minimally with the method of preparation of the specimen, and this measurement was therefore made the common factor in the comparison:

	μm
Average distance (*b*) from barb base to barbule	1·52
Average diameter of the thread (by direct measurement)	3·22
Average circumference of the thread (by calculation)	10·2
Internodal length (by direct measurement)	1·47

On the basis of air-dried material:

Maximum width of the barb (*c*) (from distance *b* and figure 9)	0·92
Calculated circumference (from *c* and figure 7)	9·0
Calculated internodal length (from *c* and figure 6)	1·08

The last two values imply that air-dried threads shrink significantly, both longitudinally and transversely, as compared with Araldite-embedded material, so that the graphs cannot be used to calculate the dimensions of corresponding internodes in undischarged and discharged threads. Indeed, it is possible that at least one of the barb dimensions specified above, namely, the maximum width of the barb, may vary with the processing of the material. A comparison was made between the maximum width of the barb, measured directly in a transverse section of an Araldite-embedded thread, and the calculated maximum width of the barb in air-dried material. In a transverse section of an arrested tip (adjacent to the section shown in figure 30, plate 21):

	μm
Measured circumference of the thread in the discharged condition	9·6
Measured maximum width of a barb	1·22

From the longitudinal section of the tip in figure 29*b*, plate 20:

Average diameter of the discharged thread	3·22
Circumference calculated from this value	10·2
In this same figure 29*b*, distance from barb base to barbule (*b*)	1·52
And the maximum width of the barb (from *b* and figure 9)	0·92

This value for the maximum width of the barb is considerably smaller than the directly measured value (1·22 μm), even though the circumference of the tip in figure 29*b* is larger than that of the thread shown in figure 30; indeed, the calculated value for the maximum width of the barb in air-dried material is almost 25% less than the value measured directly on Araldite-embedded material. This discrepancy lies outside the error of the graphs in figures 6 to 9.

(*b*) *Comparison of the length of the profile of an internode before discharge with the length after discharge*

A proportion of nematocyst capsules do not discharge completely even in distilled water; that is to say, the everted thread contains uneverted thread (Picken 1953; Robson 1953). Sections of such threads, fixed in arrested discharge, provide valuable material for determining some of the dimensional changes associated with eversion. In particular, median longitudinal sections of the dart (figure 29), and serial transverse sections from the tip of the dart backwards (figure 30), permit a more direct comparison of the dimensions of everted and uneverted regions in immediate proximity to each other. This comparison is minimally affected by systematic changes in dimensions with taper and, furthermore, the everted and uneverted regions have undergone precisely similar treatment in the preparation of the sections, and are seen simultaneously at the same magnification.

From sections such as these, it is apparent that the length of the profile of the undischarged thread—that is, the contour of the thread wall as measured with a map-measurer on a given photographic print of a section—is greater, both in longitudinal and in transverse sections, than equivalent profiles of the discharged thread. This is because, both in median and transverse sections, the profiles of the undischarged thread are not geodetics of the discharged cylindrical surface of the thread (see later, p. 147). That is to say, the profiles do not join two points on the expanded surface by a line of minimal length.

If a length of undischarged thread were sectioned transversely and then inflated to smooth out the pleats, the cut would form a zigzag edge—as can readily be shown with a folded paper model (figure 10*a*, *b*). Though certain features of the folded thread—to be mentioned later—are not represented in this model, their absence does not affect geometrical aspects now to be considered. The number of teeth formed by a transverse cut will depend on the number of helical pleats sectioned; and the angles of the zigzag, and hence the length of the profile, will depend on the pitch angle of the helical pleats. For *longitudinal sections*, the greater the pitch angle, the greater is the departure of the profile from the geodetic, and hence the longer will be the profile of the thread in section (figure 11). Towards the distal end of the thread, where the pitch angle is greatest, the length of the longitudinal profile will therefore be at its maximal value relative to the geodetic. Conversely, the profile of the undischarged thread in *transverse sections* will depart most markedly from the geodetic in sections of the dart as it emerges from the capsule. The ratio between the lengths of the perimeters of undischarged and discharged regions will here be maximal, since in this region, although the diameter of the thread is maximal, the pitch angle of the folds is minimal. The length of a profile in a section also depends on the proportion of the total surface of the thread that is incorporated into the pleats (figures 11, 12).

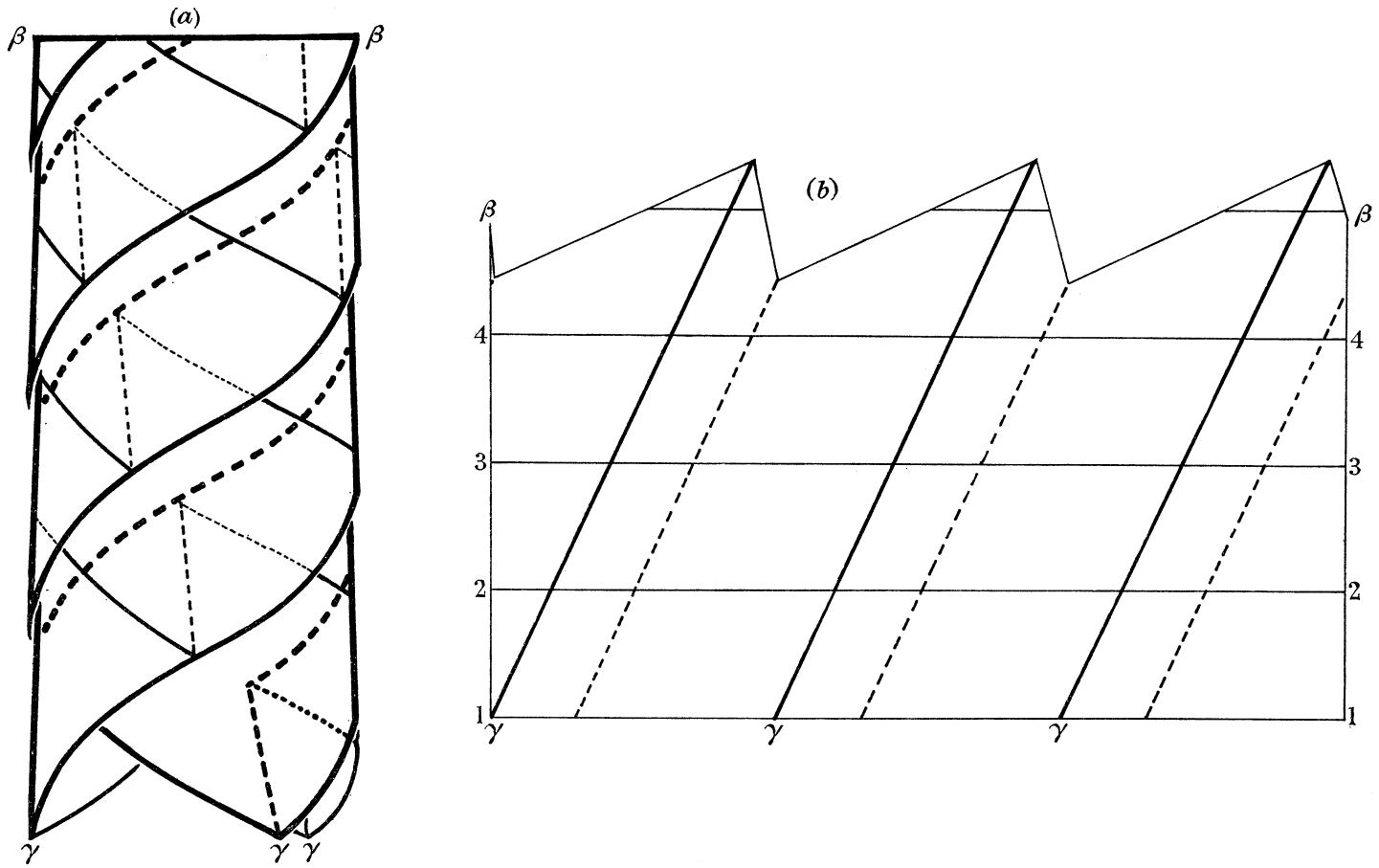

FIGURE 10. (*a*) Simplified paper model of the undischarged thread. The making of such models is described in § 5, p. 150. The cylinder is cut transversely at $\beta\beta$. The three points marked as γ result from inserting three pleats in a sheet with a straight edge. The thickest continuous lines represent the boundary of the model and the outer edges of the helical pleats. The inner edges of the pleats are in dotted lines of the same thickness as the outer edges. Exposed nodes are shown as continuous but thinner lines, and these become finely dotted and still thinner, the greater the number of thicknesses of paper through which they are seen. Except at the edge marked $\gamma\gamma\gamma$, only half the thickness of the model is shown. Since *a* is made, in effect, by pleating but not inverting a model of the discharged thread, the helical pleats are right handed rather than left handed.

(*b*) Model *a* unrolled and flattened. The transverse cut, $\beta\beta$, is transformed into the zigzag at the top of the figure. The three points $\gamma\gamma\gamma$ now lie on a straight edge. The outer edges of the three pleats are shown by the three continuous thick lines (at $\gamma\gamma\gamma$), and their inner edges by the three dotted lines. The nodes are shown by straight lines equidistant from one another and parallel to the line that includes $\gamma\gamma\gamma$. In order to accommodate figures *a* and *b* on one page, *b* is half the scale of *a*.

Thus the dimensions of similar internodes in the undischarged and discharged condition cannot be directly compared by measuring profiles in section.

The decrease in profile of the thread in transverse section on discharge may be as much as 2·5 times, whereas the decrease in profile in a longitudinal section is usually not

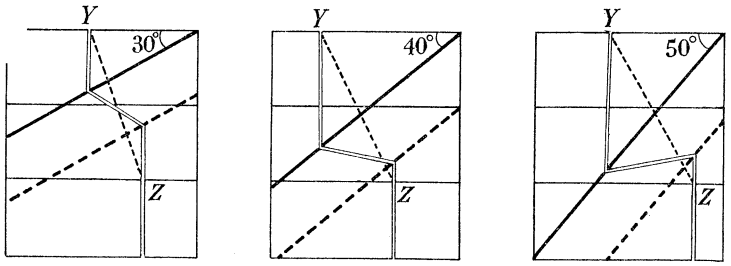

Geodetic	2·15 cm	2·23 cm	2·3 cm
Cut	2·45 cm	2·8 cm	3·43 cm
Increase in length of thread on unfolding	× 2·67	× 2·42	× 2·00

FIGURE 11. Diagrams based on paper models showing (*a*) how the lengths of geodetic and section profile (cut) increase with the pitch angle of a pleat of constant depth, (*b*) how increase in length on unfolding decreases with the pitch angle. As in figure 10*b*, outer and inner folds of a pleat are shown by thick lines, continuous and dotted respectively. Thin parallel lines crossing these are nodes. In the folded condition a cut—represented by thin double lines—has been made parallel to the long axis of the page and through the pleat, so as to join points on the nodes on either side of the pleat. The points of intersection of this cut with the nodes on either side of the pleat are marked as *Y* and *Z* after unfolding and flattening again. The dotted thin line joining *Y* and *Z* is the shortest distance between them, and if the rectangular sheet shown in the figure were part of a cylinder this line would be a geodetic. The depth of the pleat in all three models is 0·75 cm, but the pitch angle of the pleat is 30°, 40°, 50° respectively. The position of *Y* is chosen so that (i) it lies on a node, and (ii) the entire cut falls within the diagram. These same diagrams, if rotated through 90°, also show the corresponding relationships for transverse sections—assuming that the nodal lines are redrawn.

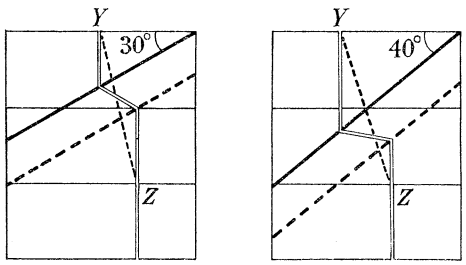

Geodetic	2·05 cm	2·15 cm
Cut	2·3 cm	2·55 cm

FIGURE 12. Diagrams based on paper models, to be compared with figure 11 (30° and 40°). The depth of the pleat here is 0·5 cm, as compared with 0·75 cm in figure 11. The difference between geodetic and length of cut is in all cases less with a more shallow pleat.

more than 1·8 times. This means that the helical pleats are at a pitch angle of less than 45° (figure 11; and figure 29, plate 20 and figure 30, plate 21).

In a tube with strictly annular folding of the surface—such as a respirator tube—which can be lengthened without rotation, the length of the profile of a fold, as seen in median

longitudinal section, is the maximum possible increase in length per pleat when the tube is extended, and the pleats obliterated. The profile of a median section of such a tube would be converted on extension to a geodetic of zero curvature, parallel to the long axis of the cylinder.

With helical pleats, however, where rotation on extension is obligatory, this simple relationship does not hold. As soon as the pleats become helical rather than annular, the equivalent geodetic becomes curved, and if the cylindrical surface is slit-up and flattened to a rectangle, the equivalent geodetic is inclined to the long axis at an angle that increases with increasing pitch angle of the helix (figure 11).

If the pitch angle of the helices is low, a relatively large increase in length of the thread will occur on discharge (figure 11), but the length of the profile in longitudinal section will be relatively small (figure 11). Conversely, in threads with helices of steep pitch angle, relatively less increase in total length will occur on discharge, but the length of the profile of the folds in longitudinal section will be far greater than the increase in length per fold. This means that the decrease in length of a profile is never simply related to the increase in length and diameter of the thread on discharge.

In a previous paper (Picken 1953, pp. 213, 214) the increase in length of the thread on discharge was estimated at between 2·5 and 3 times, and the increase in diameter at rather less than 1·5 times. In fact, as follows from the preceding exposition, the increase in length of a thread on discharge will be somewhat different in different regions of the thread, according to the pitch angle of the helical pleats (figure 11). The increase can be estimated by comparing the whorl separation of the undischarged thread with the internodal length in the everted thread. In a longitudinal section, the whorl separation is *half* the shortest distance from the base of one barb to the base of the barb immediately above it, since *alternate* whorls of barbs are in longitudinal register in the undischarged thread (figure 2*a*). Since the whorl separation varies so little with taper, an approximate estimate of the increase in length on discharge can be calculated directly from the internodal length in the discharged thread; but a more accurate calculation can be made from a median longitudinal section of a dart arrested in discharge (see (*c*) below).

In figure 29, the whorl separation is 0·5 μm, and the internodal length is 1·47 μm, so that the increase in length (1·47/0·5) is 2·93 times. This value for the increase in length is near the maximum, since the pitch angle is relatively small (28 to 29°) in this part of the thread. The diameter of the everted thread (as can be seen from the photographs in Picken and in Robson, as well as in figure 30, plate 21) is only about 50 % greater than the maximum diameter of the thread in the undischarged state, so that the change in length greatly exceeds the change in diameter. If, as appears to be the case (p. 139), the thickness of the wall of the thread is the same in undischarged and discharged threads, it is reasonable to conclude (assuming constancy of wall volume) that the area of the wall does not alter during discharge, even though markedly anisometric changes in the length and diameter of the thread occur.

(*c*) *Comparison of the area of an internode before discharge with the area after discharge*

The comparison of the area of an internode before and after discharge can only be made on longitudinal sections of a dart in arrested discharge, for it is not possible to calculate

the internodal length in the discharged thread from data given directly in a transverse section, or to use figure 6 for the purposes of such a calculation (p. 147). We need to calculate the area of an internode from the profile of its surface in longitudinal section. The profile of the undischarged internode is a complex curve, difficult to express mathematically, and the profile alters as the azimuth of the longitudinal section about the long axis changes. It is therefore convenient to use a mathematical approximation to the curve, in order to calculate the surface area of the internode.

Pappus's Theorem (Michell & Belz 1937) states that the surface area (S) described by the rotation of a curve of length l is the product of the curve and the length of the path of its centroid. The length of the path of the centroid for a complete revolution is $2\pi\bar{r}$, where $\bar{r}$ is the distance from the centre of rotation to the centroid.

Thus

$$S = 2\pi\bar{r}l.$$

For present purposes, the surface of an internode is treated as a cylinder, coaxial with the thread, of length equal to the total profile of an internode in median longitudinal section. This cylinder is generated by a straight line, parallel to the axis of the thread and passing through the centre of gravity (or centroid) of the profile.

Before discussing the procedure adopted in making this approximation, it is necessary to consider how accurate is the estimate of the surface area of an undischarged internode to be obtained by this method. The accuracy obtainable was assessed by making a simplified paper model. This consisted (figure 10*a*) of a paper cylinder with three helical pleats, so deep as almost to overlap each other, inclined at 30° to the circumference. (The construction of such a model is described in §5.) The surface area of this model in the folded condition was calculated, using Pappus's Theorem and compared with that obtained by direct measurement of the unfolded paper. The measurement of $\bar{r}$ for the model is simplified by the fact that the helical pleats lie flat against the core of the cylinder, thus reducing the angle between pleat and cylinder to zero (p. 136). $\bar{r}$ could be assumed then to be the same as the radius of the cylinder. The calculated surface area of the folded model was smaller than the surface area measured after unfolding by rather less than 4%. This suggests that the equation derived from Pappus's Theorem is a reasonably accurate approximation to apply to the folded thread of the nematocyst. If the observed agreement seems at first sight rather surprisingly good—since the surface of the thread is a screw surface rather than the surface of a solid of revolution—it must be remembered that, although this equation does not include an expression for θ (θ being the inclination of the helices), some adjustment is made for helical rather than annular folding of the wall in that, as has been shown (p. 145), the total length of a profile in section is dependent on the inclination of the helices, and it is the total length of this curve that is used in the equation.

The centroid of the profile of an internode of the undischarged thread was determined for a model of the curve made from thin fuse wire. The model was suspended at various points along its length, by means of a hair, and photographed against a background on which the vertical was marked. Tracings of the photographs were then superimposed on the original photograph of the thread, and the point of intersection of the verticals was taken to be the centroid. The internodal profile on each side of the thread was treated in this way, and the position of the axis of rotation of the curve was determined by inspection.

From figure 29*b*, plate 20:

Undischarged thread (right-hand profile)		
Length of curve (l)		4·54 μm
Distance from centre of rotation to centroid ($\bar{r}$)		0·99 μm
Area of two internodes	$(4{\cdot}54 \times 2 \times 3{\cdot}14 \times 0{\cdot}99) =$	28·2 μm^2
Area of one internode		14·1 μm^2
Undischarged thread (left-hand profile)		
Length of curve (l)		4·46 μm
Distance from centre of rotation to centroid ($\bar{r}$)		1·12 μm
Area of internode	$(4{\cdot}46 \times 3{\cdot}14 \times 1{\cdot}12) =$	15·6 μm^2
Average surface area of an internode of the undischarged thread, from two profiles		14·85 μm^2
This value is to be compared with the average surface area of the discharged thread estimated from the diameter of the discharged and everted portion in the same photograph		15·0 μm^2

There is therefore no significant change in the surface area of the thread wall on discharge.

(*d*) *Comparison of the surface-granulation pattern in undischarged and discharged threads*

As previously mentioned (p. 136), the surface of the thread wall in contact with the capsular fluid is finely granular. The spacing of the granules on discharged and undischarged regions of the arrested tip have been compared. The patterns are virtually unchanged by discharge. This observation also supports the view that no significant change in the surface area of the thread wall occurs on discharge. It must be remembered, however, that these observations are made necessarily on maximally dehydrated material.

5. The construction and geometrical properties of paper models of the nematocyst thread

Straight lines (representing the nodes) spaced at a constant distance (representing the internodal distance) are drawn parallel to one edge of a rectangular sheet of paper and numbered in sequence on the two sides (figure 13*a*). This edge is now divided into three equal lengths, from the right-hand ends of which three straight lines are drawn at an angle of 65° to this same edge. These three oblique lines represent the sites of the outer folds of the three helical pleats; they run parallel to the helical rows of barbs. Since the pleats of successive helices almost (or just) overlap in the undischarged thread, the depth of each pleat must be approximately one-third of the distance between the oblique lines representing the outer folds of the pleats. Dotted lines at one-third of the distance between two oblique lines mark the inner fold of the pleats. If now the sheet is folded, so that the direction of folding along continuous lines is the opposite of that along dotted lines, and if the pleats are maximally flattened, it is converted to the shape shown in figure 13*b*.

It is plain that the action of making a pleat displaces the nodes, so that if the two sides

of the original sheet are compared, previously corresponding nodes are no longer in register. When corresponding nodes are again brought into register, by coiling the pleated sheet about a new axis, at right-angles to the line joining the two ends of the same node in the pleated condition, the original axis—represented by the line of suture of the two edges —is a helix of high pitch-angle. The pleats themselves now form helices at an inclination of *ca.* 30 to 35°, instead of 65° in the unpleated condition. This change from 65° to 30 to 35° depends on: (1) the number of pleats, and (2) the ratio of the depth of each pleat to the circumference—assuming (as observation suggests) that the inclination of the barb rows in discharged threads is effectively constant. Models with a single pleat show how the pitch angle of the pleat changes with the ratio of the depth of the pleat to the circumference.

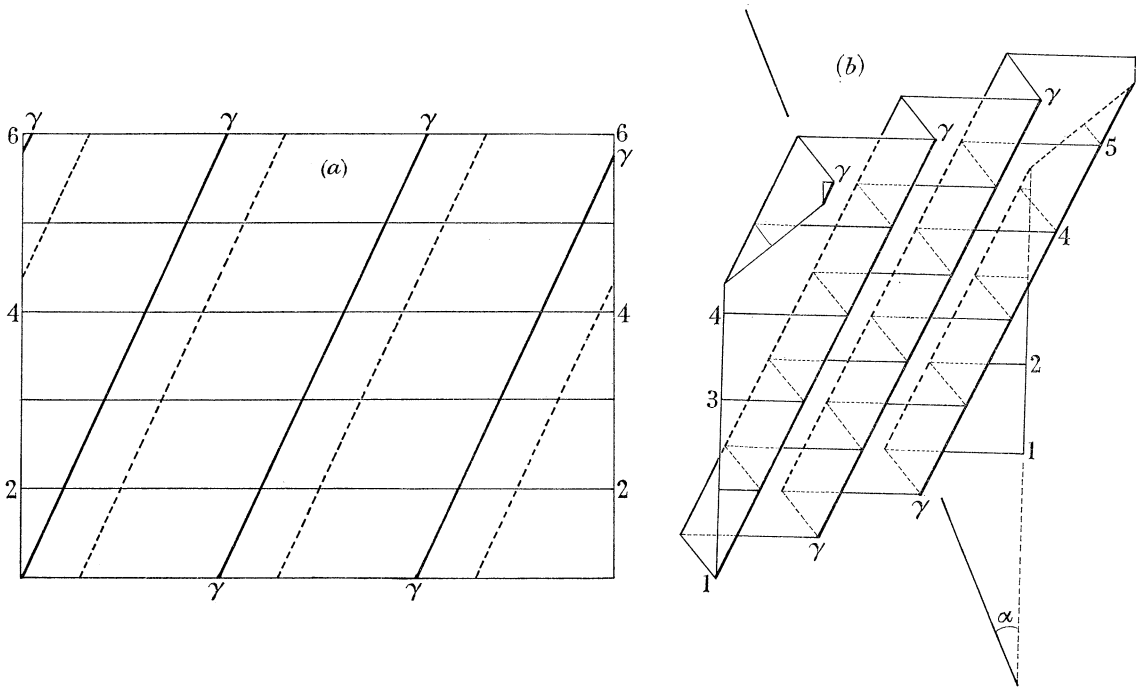

FIGURE 13. (*a*) Sheet of paper ruled, preparatory to making a model of the undischarged thread. The conventions are as in figure 10*b*. The nodes are numbered in sequence on the two sides of the sheet.

(*b*) The sheet has been pleated and is shown to the same scale and in the same orientation. The interrupted diagonal line is the axis round which the pleated sheet must be rolled if corresponding nodes are to be brought into register. The angle between this and the side of the sheet is α.

In figure 14, R and r represent the same point on a node (the circumference of a cylinder). When a pleat of depth p is inserted, R moves to R_1, and the line joining R_1 to r represents the base of the cylinder produced by superimposing R, R_1 and r. The new inclination of the pleat (θ) will be $\theta' - \alpha$, where θ' is the original inclination and α is the angle between the old and new lines Rr and R_1r. The value of α can be calculated, knowing p and the circumference, c, by dropping a perpendicular from a point T on Rr to R_1. Let the distance RT be x and the distance R_1T be v. Since the line $RR_1 = 2p$ and is the normal to the

outer edge of the pleat, $\angle R_1RT = 90° - \theta' = 25°$. It can be shown (Appendix, p. 164) that:

$$\tan\alpha = \frac{\cos\theta'}{(c/2p) - \sin\theta'}.$$

Thus $\tan\alpha$ varies with the depth of the pleat (p) and inversely with the circumference (c). If the ratio p/c is constant, α also is constant. Thus the pitch angle of the pleat decreases as α increases, that is, as the ratio p/c increases.

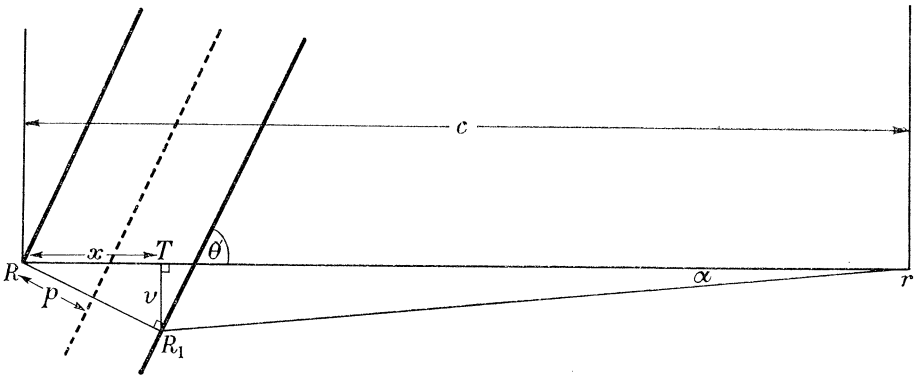

FIGURE 14. Diagram showing the relationship between α, depth of pleat (p) and length of circumference (c). R and r are the same point on the circumference of a cylinder. Inserting a pleat of pitch angle θ' and depth p at R, R moves to R_1. The straight line joining R and R_1 is perpendicular to the fold of the pleat passing through R. α is the angle between the original circumference, Rr, and the new circumference R_1r. TR_1 is a perpendicular to Rr passing through R_1. (See text.)

With more than one pleat, α_n (where n is the number of pleats) increases, but not as a simple multiple of α. If, for example, with one pleat α is 6°, with two, α_n will be 14·5°, and with three, 30°. This is because inserting a further pleat changes the pitch angle of any previous pleat and also reduces the circumference.

Observations on the undischarged thread have shown that the pitch angle of the pleats increases with decrease in circumference. If the circumference were reduced, without change in the ratio of pleat depth to circumference, we should expect (from the equation previously derived) that α, and hence the pitch angle of the pleats, would remain unchanged. Since, however, the pitch angle is observed to increase from the attachment region towards the free end of the thread, this can only mean that the depth of the pleats simultaneously diminishes more rapidly than the circumference, and the value of the ratio p/c falls. In parts of figures 19 and 29 it can be seen that, whereas there is no overlap between successive pleats in the narrower thread (figure 19), overlap occurs in the wider thread (figure 29), even though the whorl separation (p. 137) is the same in both.

At present, no reason can be given for the observed constancy of whorl separation throughout the length of the undischarged thread. Combining the graphs in figures 6 and 7, we obtain a straight-line relationship between circumference and internodal distance along the discharged thread. As the circumference of the thread diminishes, therefore, the whorl separation can only remain constant in the undischarged thread if less of the thread wall participates in the formation of pleats. At the same time, the pitch angle of the pleats

is observed to increase with reduction in diameter. This increase in pitch angle again implies a reduction in the depth of the pleat. Whether this reduction of itself suffices to provide sufficient wall membrane outside the pleat to preserve constancy of whorl separation is unknown. Clearly, however, it would be possible to achieve this constancy by reducing the proportion of the surface in the folds *more* than the internodal surface is reduced as the diameter diminishes.

6. Comparison of models and thread

An accurate model of the folded thread cannot be made by merely folding a sheet of paper or other inextensible material. Indeed, because paper is inextensible, it is impossible to fold a *cylinder* of paper into the shape of the model. The models were all made by first

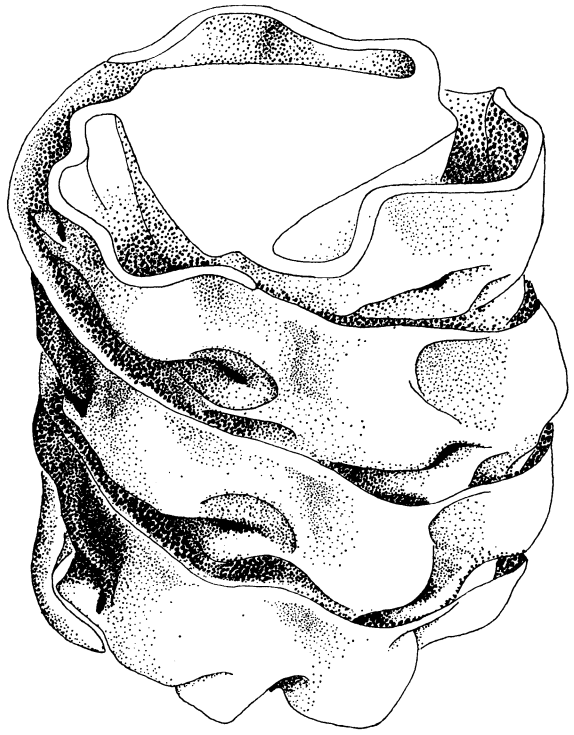

FIGURE 15. Stereogram of a short length of undischarged nematocyst thread from a large holotrichous isorhiza of *Corynactis viridis*, prepared from a wax model. The model was constructed from serial electron micrographs. The clear triangle at the top outlines the core. The barbs comprising the core would be oriented with their tips pointing downwards. Three pleats arise from the triangle. Their helical course is shown in three-dimensional relief. The ends of barb-pockets and the fluting of the surface are suggested by shading.

folding the sheet and then rolling it into a cylinder. The pleats of the paper models are maximally flattened and lie flat against the core (p. 136) of the pleated cylinder (in models, without barbs). In the undischarged thread, however, the pleats are not maximally flattened and do not lie against the surface of the core (figure 15); their profile in transverse section is described on p. 136. Longitudinal sections (figures 19, 29; plates 14, 20) show that they are inserted on the core at an angle varying between 90° and 30° to the axis—at the latter extreme they are almost parallel to the axes of the barbs. This means

that the pleats are inserted on the core like the thread of a carpenter's screw, in the sense that they stick out from a central core. A line following the free edge of such a pleat (or of a screw thread) must be longer than a line following its insertion. In turn, this implies that it is impossible to convert such a pleated surface to a cylinder without local deformation. This has been tested (*a*) by covering a large screw with a rubber balloon previously marked with a rectangular grid of inked straight lines, and (*b*) by examining the properties of a membrane of polyvinyl chloride, deposited on a wax screw, after melting the waxen form. In (*a*) it was observed that the rectangular grid is stretched at the crests of the screw thread and contracted in the troughs, while in (*b*), any attempt to inflate the screw surface to a cylinder resulted in buckling in planes at right-angles to the plane of the screw thread.

The fact that the pleats of the nematocyst thread are inserted at an angle to the axis of the core implies, therefore, that they cannot be obliterated during discharge without local deformation of the wall. As shown in figures 19 and 29, plates 14 and 20, however, the plane of the pleat (as seen in median longitudinal section) is curved rather than flat; that is to say, the angle between the plane of the pleat and the axis decreases, as one moves along the pleat from the core towards its free edge, until the edge of the pleat is often parallel to the axis. The configuration of the pleats of the thread is therefore intermediate between the condition of the thread of a screw and the condition of the pleats in the paper-models. The degree of distortion in the plane of the surface necessary to convert an object in the form of the paper models to a cylinder would be less than the deformation necessary to transform the undischarged nematocyst thread to a cylinder, and this in turn is less than the deformation necessary to convert a simple screw surface to a cylinder. Since paper is inextensible, the pleats of paper models cannot be lifted from the surface of the core—an operation presupposing stretching of the surface. A simple folded sheet of paper, rolled into a cylinder, cannot therefore be made to assume the configuration of the undischarged thread.

The transformation during discharge, from a folded screw-like surface to a cylindrical surface, must therefore result from a non-homogeneous deformation of the surface. As demonstrated in §(*c*) (p. 148), this non-homogeneous deformation involves little or no change in area of the surface. Furthermore, notwithstanding the absence of an overall change in area, there must be local anisometric changes in dimensions on the submicroscopic scale, in parallel with gross anisometric changes in dimensions §(*b*) (p. 148), if the helically pleated tube is to become a cylinder.

7. The hygroscopic properties of the thread and the question of reversibility of discharge

Undischarged threads may be isolated without change by cutting off the tip of a capsule under liquid paraffin, pulling out the thread with a micro-needle, and removing the paraffin by washing with a suitable volatile solvent (for example, benzene). It is plain from the behaviour of such threads, isolated as far as possible in the dry state, that the nematocyst thread itself is a hygroscopic mechanism, magnifying by its structure the ultramicroscopic dimensional changes that occur when water molecules (as vapour or as liquid) are admitted to the system. As water vapour is taken up, the undischarged thread lengthens

and partially untwists. If the process of hydration is limited to the uptake of water molecules from a saturated atmosphere, the mechanical consequences of hydration appear to be completely reversible, and the undischarged thread can be made to lengthen (with untwisting) and to shorten again (with twisting) at will. Unpublished observations by Dr Elaine Robson have shown that isolated, undischarged threads in aqueous solutions of sucrose assume lengths that decrease as the concentration increases, and that this decrease is to some extent reversible; but the practical difficulties of handling, measuring and irrigating such threads have so far precluded accurate measurement of changes in length. If instead of breathing on such isolated threads, they are flooded with water and then allowed to dry out, they do not shorten and coil as they dry. This non-reversibility of the expanded state of the thread in distilled water is associated with flattening on drying out. The reason for collapse may be that the surface of the evaporating water droplet compresses the still hydrated thread as it contracts, and that by the time the level of hydration in the thread has reached a value below saturation, the thread has been so deformed by compression that it can no longer shorten.

It is certain that even the everted state of the thread is not completely irreversible. In a single instance where an isolated capsule had been caused to discharge by being breathed on, it was observed that the dart withdrew somewhat as the capsule and thread dried out again. This withdrawal of the dart implies reconversion of the thread to the uneverted condition and its progressive withdrawal down the cavity of the tube.

8. The process of discharge and eversion

In spite of the capacity of lengths of isolated, undischarged nematocyst thread to expand in distilled water, it is clear (from observations with the light microscope) that in the discharge of an intact, isolated capsule in distilled water, the undischarged thread (emerging as a core to the expanded, everted thread as it leaves the capsule) does not undergo appreciable dilatation before it becomes the tip. This must mean that the speed of exit of the thread from the capsule exceeds the speed at which water can penetrate into the thread itself during discharge. A number of observations suggest, indeed, that the usual picture of orderly discharge depends on a balance between rates of inward diffusion of water into all parts of the system and of orderly dilatation with progressive unfolding of the various parts of the thread. Though the forward movement of the dart may cease from lack of water, for example, changes in the discharging thread may continue for a while. This is shown by light microscope observations on isolated capsules discharged on a microscope slide in a drop of sea water small in relation to the volume of the capsule. If the capsule begins to discharge, it is observed that the dart ceases to progress when all the water has been absorbed, but the undischarged regions of the thread enclosed by the everted thread continue to rotate in a counter-clockwise direction (looking from the capsule towards the dart), at first rapidly, then progressively more slowly until movement finally ceases altogether. During this rotation, part of the undischarged, rotating core may even be seen to move backwards into the capsule—the thread may be said to 'back-fire'. As a result of such a back-fire, the capsule becomes filled with coils of partly discharged (but uneverted) thread.

It seems highly improbable that this rotary movement might be due to the momentum of the core; rather do the observations suggest that the processes leading to discharge are affecting all parts and are not necessarily halted simultaneously throughout the system when the dart ceases to advance.

A converse situation, in which the speed of exit from the capsule seems to exceed the speed of forward movement of the dart, can often be observed when the dart region (but not the capsule) of partially discharged capsules in a dried smear is rehydrated. Under these conditions, the thread ruptures at the dart, and coils of the undischarged core are thrown out, dilating and coiling round each other (but not everting) to form a sort of 'palm tree' at the arrested tip. One can only speculate as to the reason for rupture of the tip under these conditions—a contributory factor may be that the discharged thread becomes very brittle when dried—but it is clear that normal discharge presupposes the continuing forward movement of the dart, and the regular forward extension of the tube of everted discharged thread, up which the undischarged thread travels.

Leaving light microscope observations and turning to electron micrographs, the appearance of an arrested dart, sectioned longitudinally, suggests that the dimensions of the undischarged portion of the thread remain unchanged up to the dart (figure 29, plate 20): the barbs retain their tight packing, and the helical pleats appear to be unaltered. All that has happened, as far as can be seen, is that the wall on which the barbs forming the dart are inserted is reflected back over the undischarged regions of the thread. Inasmuch as the spacing of the barbs remains the same, even *distal* to the level where eversion of the wall is occurring (figure 29), and furthermore, the region of the wall undergoing eversion does not appear to be inflated by its contents, this photograph (and others of arrested tips) at first sight suggests that, whatever the mechanism of eversion may be, it cannot consist in a local inflation of the contents at the tip of the advancing thread.

A further aspect of discharge revealed in this and other micrographs is the smallness of the distance (200 to 500 Å) between the discharged wall and the undischarged thread. This distance is very much smaller than it appears to be in photomicrographs made with the light microscope.

It is possible, however, that the appearances at the dart, and the small distance between uneverted and everted regions, are to some extent artifacts. If back-firing (p. 155) occurs during fixation, the real dimensions both at the tip and elsewhere will be changed.

If the distance between the undischarged core of thread and the outer cylindrical wall of the discharged thread appears smaller than expected in electron micrographs, it may under certain conditions appear to be very much enlarged. This is particularly noticeable during the slowed discharge of capsules in a nearly saturated solution of magnesium chloride, for example. Under these conditions, the diameter of the undischarged thread is reduced, and the space between discharged wall and internal thread is conspicuously greater than in threads discharging under normal conditions. This feature of slowed discharge is shown in films of the discharge of capsules in solutions of neutral red made by Weill (1961). It may be pointed out, that the uptake of water molecules by the undischarged but discharging thread is likely to be considerably influenced by its state of torsion (as with a twisted dish-cloth!), which in turn will depend on shearing forces in the capsule and in the space between the undischarged and discharged regions of the thread.

Robson (1953) observed that the undischarged thread rotates in a counter-clockwise direction (looking from the capsule towards the dart) during discharge; this direction of rotation had been predicted from the geometry of the thread. Since the pleats in the thread wall are left-handed helices, rotation in a counter-clockwise direction may be expected to tighten the helices (by shear or friction between undischarged and discharged regions), and thus to reduce the diameter of the undischarged thread, increasing the space between wall and thread. Conversely, when back-firing occurs, the dart having ceased to advance, the uneverted thread will continue to rotate in the same direction as before, and the space between the expanded, everted thread and the undischarged thread will diminish. The fact that the diameter of a helically pleated cylinder varies inversely with torsion may be an important self-regulatory property of this system.

In order to determine the dimensions of everted and uneverted regions in normal discharge, it will be necessary to make measurements on photomicrographs obtained by high-speed, high-resolution cinematography. Accurate knowledge of these is essential to any calculation of the shearing forces generated as the undischarged region moves distally and rotates within the everted tube.

The similarity in appearance of the undischarged thread, as it travels up the discharged portion, to the as yet undischarged thread in the capsule, suggests that in normal discharge, the undischarged portion may be being propelled up the tube of discharged thread as a helical piston, displaced by the incompressible, dilating working-substance in the capsule. Though the pressure exerted by the swelling capsular fluid on the tube wall and on the piston will be equal, the force acting on the latter will be greater if, as seems to be the case, the undischarged thread almost fills the tube of the discharged thread.

Notwithstanding the unchanged appearance of the ascending core of the thread in *normal* discharge, partially discharged capsules, dried on a slide until the capsule is wrinkled, will resume discharge if a minute drop of water is deposited on the tip, and will often continue to discharge to completion (with or without the formation of a 'palm tree') even though the water meniscus does not reach the capsule—as shown by the fact that the capsule remains wrinkled. This can only mean that the partially discharged thread itself contains all the necessary machinery for complete discharge, though the discharge may well be abnormal.

9. Discussion

The evidence of electron micrographs has brought about a change in outlook on the process of nematocyst discharge. It has become plain that anisometric dilatation of the thread on hydration does not necessarily imply anisotropy in molecular texture. The dehydrated thread is seen to be complexly folded at a supramolecular level of magnitude, intermediate between molecular and microscopic dimensions; and it is the unfolding of this supramolecular structure which results in anisometric dilatation. The original argument from the geometry of discharge (as observed under the light microscope) to the hypothesis that the material of the thread was ordered on left-handed helices of low pitch angle (right-handed after eversion), erred in the assumption that it was necessarily chain molecules or micells that were oriented in this way, and that anisometric dilatation was due to the partial separation of these by water of hydration. If the oblique lines in figure 7 (*a*)

(Picken 1953, p. 152) are interpreted as helical pleats, the transformation on hydration may still be represented (neglecting changes in diameter) by the accompanying figure 7 (*b*) but the interpretation of this transformation has changed.

The chief reason at that time for assigning a principal role to anisotropic swelling properties of the thread wall itself was the *experimentum crucis* of Robson (1953) which, like other crucial experiments, did not necessarily mean what it was supposed to mean. The experiment showed that a detached length of undischarged thread extends without eversion when it is hydrated. The undischarged thread therefore has intrinsic powers of extension, independent of its connexion with the swelling contents of the capsule. The conclusion from this—supporting the hypothesis of Will (1914)—that these intrinsic powers reside in the thread wall, ignored the fact that, as the electron microscope has shown, the cavity of the undischarged thread is filled with material that may be osmotically active, as is the capsular fluid. If the thread wall were to behave as a membrane semi-permeable to the molecules of a concentrated, osmotically active substance in its cavity, the extension of a length of undischarged thread on hydration might be due, in part at least, to the swelling of this substance. When electron micrographs also showed that the wall is greatly folded in the undischarged condition, there was no longer any reason to interpret anisometric swelling exclusively in terms of anisotropic molecular arrangement, since, as we have seen (p. 150), the area of the thread wall does not alter significantly between the dehydrated inverted, and the hydrated everted, condition.

The present study raises a number of questions that cannot as yet be answered, such as: how does the thread develop and come to assume its characteristic configuration in the undischarged condition? Is the folded surface produced by buckling an originally cylindrical surface? Or is it a membrane deposited in the folded configuration without distortion?

The simplest hypothesis would seem to be that the wall-membrane, formed initially as a cylindrical extension of the wall of the primary capsular vacuole, subsequently becomes buckled. As yet it is impossible to decide whether this extension is formed primarily about an external process emerging from the vacuole, or as an invagination into the vacuole; the electron microscope evidence so far seems to favour the former view. From earlier light microscope studies, it appears certain that the barbs are formed at a relatively late stage. The hygroscopic properties of thread and capsular fluid imply not only that materials with a quite exceptionally high affinity for water are being elaborated during the development of the nematocyst, but also that these are in an extremely dehydrated condition by the time the nematocyst is mature. This means that water must be actively withdrawn from the capsule during the final stages of development. If at this time the thread wall is semi-permeable and has a finite area below which it cannot contract, the consequence of removing water from the system must be to buckle the thread wall, if the contents of the thread behave—in spite of terminal continuity with the capsular fluid—as the fluid in an osmometer.

It must be borne in mind that the folding of a membrane necessarily implies the stretching of its substance on the convex side of the fold and its compression on the concave side in those regions where the curvature is greatest; a membrane can only be folded if its rigidity does not preclude these reciprocal deformations. The number of

circumferential folds produced by elastic buckling will depend on the ratio between the thickness of the cylindrical wall and the radius of the cylinder (Timoshenko 1936). The buckling of a tube of protein, such as is the nematocyst thread, might be expected to be *plastic* rather than *elastic*, however. Holland (1960) has shown that for a tube of aluminium of the same ratio of thickness to diameter as the nematocyst thread (accepting values of 350 Å (thickness)/5 μm (diameter) for the latter), the pressure required to produce a buckled cylinder with circumferential lobes in triadic symmetry is less than that needed to produce a pattern of annular folds or circumferential lobes with tetradic symmetry. (See also Pugsley & Macaulay 1960). It must not be forgotten that the barbs themselves form a central axis with conspicuous triadic symmetry, and this might predispose the system to threefold symmetry. Though the tips of barbs of the same whorl are closely adpressed on each other, they are not, strictly speaking, close-packed and can be brought into closer-than-normal contact by torsion of the thread. The bases of the barbs, however, are at all times distributed in a regular hexagonal pattern, even though widely separated from each other in open array on what is, in the undischarged thread, an imaginary cylindrical surface. Clearly, however, barbs are not essential to the generation of pleats by buckling.

If the volume of the fluid contents of the thread were progressively reduced by dehydration, the wall might be expected both to fall into a small number of pleats and to accommodate itself between and around the barb bases and the barbs, so that the volume enclosed was minimal, subject only to the qualification that the volume enclosed between the two surfaces of a pleat cannot, apparently (figures 19, 20, 21, 29, 30, plates 14 to 21), be reduced to zero.

The extreme regularity of folding of the undischarged thread implies either an extreme uniformity of mechanical properties of the thread wall throughout its structure, as well as complete homogeneity in its environment and in the forces acting on it, or (and perhaps as well) a built-in constraint, either inherent in the molecular structure of the wall or imposed by the barbs.

In this connexion, the condition of insect tracheae and tracheoles may be recalled. These tubular structures, ranging from 0·2 μm to 1 mm or so in diameter, are buckled in a highly regular fashion, with either annular or helical pleats (the latter of very low pitch angle). These arise, according to Locke (1958), because the cuticular surface of the tube expands in area while the two ends are fixed. The resulting buckling is the equivalent of compressing a cylinder from the two ends, while its surface remains of constant area. Here again, the regularity of the pleating exceeds that to be anticipated in any macroscopic system induced to buckle under the action of forces externally applied. In the nematocyst thread, as in the trachea, the stress necessary to generate helical rather than longitudinal or transverse pleats will presumably be only a small fraction of the total stress.

The absence of significant change in area on discharge implies that, if the folded thread is produced by buckling, areas of compression must cancel out areas of extension when hydration occurs, so that the equilibrium surface is a cylinder. Should the thread wall be laid down in the folded condition, without distortion, so that the folded condition is strain-free, some molecular rearrangement must occur during discharge, if the final surface is to be cylindrical. On the whole, electron-microscopic evidence at present supports the view that the undischarged thread begins development as a cylinder.

Nevertheless, the accuracy with which details of the characteristic barbs of each type of nematocyst are duplicated throughout the barb population of the thread would seem to imply great precision in the placing of individual molecules of specific proteins. This suggests that it would not be impossible for the membrane to be *deposited* in the configuration it displays in the undischarged state, given a sufficient number of specific proteins. As yet, however, it seems improbable that this is in fact the method by which the shape of the pleated membrane is determined.

So far, electron-microscopic studies have thrown little light on the finer structure of the thread wall (p. 139), and what little is known does not help in deciding between the alternatives of buckling or strain-free deposition. The reversible extensibility of the discharged, hydrated thread suggests that its molecular structure might be that of a rubber-like elastomer, but the slight positive birefringence with respect to the long axis implies some ordered structure other than that of a rubber-like membrane with molecules randomly oriented in two dimensions. One possibility is that the discharged thread has a crossed-fibrillar texture, comparable to some extent with that of the basement membrane of the nemertine epithelium (Cowey 1952) or of the cuticle of *Ascaris* (Harris & Crofton 1957). A cylinder of submicroscopic fibrils arranged as a network of crossed geodetics and embedded in an amorphous, rubber-like matrix, would exhibit the observed long-range reversible extensibility of the wet thread—up to *ca.* 100%. It would also be able to assume the configuration of the anhydrous, undischarged thread without change in area, if 'racking' of the fibrils permitted local changes in the angle of the crossed lattice above and below the mean value (90°) in the unstressed, discharged state. From the observed continuity between capsule wall and thread, it is at least possible that the thread, like the capsule wall, has effectively a crossed-fibrillar texture. As shown in figure 26, plate 18, the attachment scars of the barbs reveal a pattern of two periodicities. There is as yet no evidence, however, that this observation is relevant to the texture of the wall.

Even though a regular molecular arrangement in the wall may not assist in the process of discharge, it is difficult to believe that swelling of the wall plays no part in extension. Electron micrographs have shown no difference in thickness between the undischarged and the discharged thread wall, but both membranes have necessarily been dehydrated in the same way in preparing the material for sectioning, and it seems unlikely that the wall exhibits in reality no increase in thickness on hydration—as do a majority of biological membranes. An increase in thickness would assist in the process of ironing-out folds, just as in a piece of crumpled cellophane thrown into water.

The observed asymmetry of individual barbs excludes, at first sight, any interpretation of their formation as a 'crystallization out' of a single molecular species. It is important to note that this asymmetry is a property of a single barb—as can be observed in barbs in isolated positions on the thread (figure 28, plate 19; p. 140). Since the speculations on the development of nematocysts made in 1953, several important changes have occurred in the general picture of the relationship between various molecular species (in particular protein species), and the ultramicroscopic, supramolecular structures to which they give rise.

It is now clear, for example, that a number of different protein species participate in the formation of such a relatively simple submicroscopic structure as the bacteriophage particle (see, for example, Stent 1963). In relation to the tailed T4 phage, it had already

become clear from the work of Brenner *et al.* (1959) that there exists a striking analogy between the transformation of the phage tail and that of the nematocyst thread (Picken 1961). The elongated phage tail shortens as a result of the re-packing of helically disposed, molecular protein units as a helix of lower pitch angle. This shortening, in approximating the two ends of the tubular sheath of the tail, drives the internal core through the bacterial cell wall and so admits the phage *DNA* to the interior of the bacterium. More recently Kellenberger & Boy de la Tour (1964) have offered molecular interpretations of the tail structure and behaviour that are even more strikingly reminiscent of the nematocyst thread. Thus the tail sheath, like the pleated nematocyst thread, is a multistranded helix of at least three helical bands, and in the extended condition the pitch angle is 60°. This angle changes to 30° when the triple helix shortens. Shortening is interpreted as a consequence of re-packing subunits, brought about by transition of these from form *A* to form *B*. Both extended and shortened configurations are 'multistranded isoaxial helices', and the re-packing resulting in shortening is supposed to be due to the unmasking of previously masked chemically active groups on the surface of the subunits which form chemical bonds with each other and constitute a new array.

The mode of operation of the phage tail cannot, however, be precisely the converse of a diminutive nematocyst thread discharging, since in the contracted condition the nematocyst thread is narrower as well as shorter than in the expanded condition. Indeed, the nematocyst could not work as it does, with the undischarged portion of the thread travelling up the cavity of the discharged thread, unless the diameter of the latter were greater than that of the former.

This same paper by Kellenberger & Boy de la Tour also discusses the general problem of self-assembly of submicroscopic structures from 'design-specific subunits' with or without the intervention of certain factors termed 'morphopoietic principles'. If we attempt to formulate the problems of the formation of the nematocyst thread in such terms, it does not seem possible that a *single* species of protein subunit should generate the thread wall by self-assembly, since the wall appears heterogeneous in transverse section. On the other hand, there seems no reason why the principle of self-assembly should not operate with more than one type of protein subunit.

If an asymmetrical object, such as a barb, is to be formed by the spontaneous aggregation of specific molecules at specific sites, therefore, it would appear that several protein species must participate. It therefore seems likely that microscopic structures of the complexity of a nematocyst presuppose the synthesis of many different types of protein molecules, even though these may be chemically interrelated. In so far as observations have been made on types of nematocysts other than the holotrichous isorhizas in *Corynactis* (for example, spirocysts and microbasic mastigophores) these show that the types differ in the structure of the capsule wall, of the barbs and in the pleating of the thread, down to the smallest structural levels that can be discriminated. This state of affairs can only mean (it is submitted) that a host of different proteins participate in the elaboration of each type of nematocyst. This implies that a far larger number of specific building blocks are synthesized than was previously envisaged. It will be remembered that these different expressions of the genotype are associated (in *Hydra* at least) with the number of simultaneous divisions undergone by the primary interstitial cell (Lehn 1951).

On the other hand, the fact that data from widely differing sizes of nematocysts (holotrichous isorhizas) fall on the same straight-line graphs (figures 6 to 9) implies that differences in the quantities of materials synthesized by a particular cnidoblast lead to no conspicuous changes in the relative proportions of the structures generated.

In interpreting the genesis of biological fine structure, it is now clear not only that a much larger number of molecular species can be invoked, but also a far greater specificity of intermolecular interaction than seemed at one time feasible.

Summarizing, then, our present view of the nature of the nematocyst as a piece of machinery, and of the aspects of its structure and function that urgently require further investigation: the nematocyst is a hygroscopic mechanism, every part of which responds with changes in dimensions to the addition or removal of water molecules. 'Normal discharge' of an isolated capsule in distilled water is the sum of changes in the volume of the capsular fluid (including that fraction enclosed in the cavity of the thread) and in the shape of the pleated thread wall, but not significantly in its area. 'Normal discharge' depends on a 'normal' balance of the speeds at which these various changes occur.

In order to understand more fully, and ultimately to measure, the forces acting during discharge, it is above all necessary to know the exact dimensions of all parts of the system during the process of discharge, from start to finish. Although the area of the thread wall remains approximately unchanged by discharge, the pleated surface cannot be inflated to a cylinder unless deformation as well as unfolding occurs. We have already stressed the importance of a re-examination by modern techniques of the development of nematocysts, without which many questions relating to the pleated condition of the undischarged thread cannot be answered. In spite of current studies of nematocyst toxins and the products of hydrolysis of capsule and capsular fluid, virtually nothing is known as yet of the physical chemistry of the capsular fluid and thread contents or of the molecular constitution of the intact capsule, thread wall and barbs. In the absence of this information, it is prudent to postpone discussion of the mechanism of discharge.

We wish to acknowledge our debt to the following colleagues with whom this work was discussed at various stages: to Dr A. E. Dorey who made valuable suggestions at all stages; to Dr K. E. Machin and Dr Elaine A. Robson who commented on the typescript; and to Dr J. M. T. Thompson and Mr C. R. Calladine who advised us on buckling and related matters. We are also indebted to Dr Elaine A. Robson for allowing us to quote her unpublished observations. During the period in which this research was carried out, one of us (R.J.S.) was a Research Fellow of Peterhouse.

References

Brenner, S., Streisinger, G., Horne, R. W., Champe, S. P., Barnett, L., Benzer, S. & Rees, M. W. 1959 Structural components of bacteriophage. *J. mol. Biol.* **1**, 281.

Bretschneider, L. H. 1949 A simple technique for the electron-microscopy of cell and tissue sections. *Proc. K. Acad. Wet. Amst.* **52**, 654.

Carlgren, O. 1940 A contribution to the knowledge of the structure and distribution of the cnidae in the Anthozoa. *Acta Univ. lund.* **36**, No. 3, 1.

Chapman, G. B. 1961 The fine structure of the stenoteles of *Hydra*. *The biology of* Hydra, p. 131 (ed. H. M. Lenhoff and W. F. Loomis). University of Miami Press.

Chapman, G. B. & Tilney L. G. 1959 Cytological studies of the nematocysts of *Hydra*. I. Desmonemes, isorhizas, cnidocils, and supporting structures. II. The stenoteles. *J. biophys. biochem. Cyt.* **5**, 69, 79.

Cowey, J. B. 1952 The structure and function of the basement membrane muscle system in *Amphiporus lactifloreus* (Nemertea). *Quart. J. micr. Sci.* **93**, 1.

Cutress, C. 1955 An interpretation of the structure and distribution of cnidae in the Anthozoa. *System. Zool.* **4**, 120.

Hand, C. 1961 Present state of nematocyst research: types, structure and function. *The biology of* Hydra, p. 187 (ed. H. M. Lenhoff and W. F. Loomis). University of Miami Press.

Harris, J. E. & Crofton, H. D. 1957 Structure and function in the nematodes: internal pressure and cuticular structure in *Ascaris*. *J. exp. Biol.* **34**, 116.

Holland, P. B. 1960 Crumpling of thin walled tubes (unpublished).

Kellenberger, E. & Boy de la Tour, E. 1964 On the fine structure of normal and 'polymerized' tail sheath of phage *T4*. *J. ultrastruct. Res.* **11**, 545.

Lehn, H. 1951 Teilungsfolgen und Determination von I-Zellen für die Cnidenbildung bei *Hydra*. *Z. Naturf.* **6**b, 388.

Locke, M. 1958 The formation of tracheae and tracheoles in *Rhodnius prolixus*. *Quart. J. micr. Sci.* **99**, 29.

Luft, J. H. 1961 Improvements in epoxy resin embedding methods. *J. biophys. biochem. Cyt.* **9**, 409.

Michell, J. H. & Belz, M. H. 1937 *The elements of mathematical analysis*, **2**, 868. London: Macmillan.

Picken, L. E. R. 1953 A note on the nematocysts of *Corynactis viridis*. *Quart. J. micr. Sci.* **94**, 203.

Picken, L. E. R. 1961 Molecular biology and the future of zoology, *The cell and the organism*, p. 90 (ed. J. A. Ramsay and V. B. Wigglesworth). Cambridge University Press.

Pugsley, Sir A. & Macaulay, M. 1960 The large-scale crumpling of thin cylindrical columns. *Quart. J. Mech. appl. Math.* **13**, 1.

Robson, E. A. 1953 Nematocysts of *Corynactis*: the activity of the filament during discharge. *Quart. J. micr. Sci.* **94**, 229.

Slautterback, D. B. 1961 Nematocyst development. *The biology of* Hydra, p. 77 (ed. H. M. Lenhoff and W. F. Loomis). University of Miami Press.

Stent, G. 1963 *Molecular biology of bacterial viruses*. San Francisco and London: W. H. Freeman.

Timoshenko, S. 1936 *Theory of elastic stability*, p. 480. New York and London: McGraw-Hill.

Weill, R. 1930 Essai d'une classification des nématocystes des cnidaires. *Bull. Biol. Fr. Belg.* **64**, 141.

Weill, R. 1934 Contributions à l'étude des cnidaires et de leurs nématocystes. *Trav. Sta. zool. Wimereux*, **10**, **11** (I, II).

Weill, R. 1961 Presentation of film at the International Congress of Zoologists, Washington, D.C., U.S.A.

Westfall, J. A. & Hand, C. 1962 *5th Int. Congr. Elec. Micr. Philadelphia*, **2**, M. 13 (ed. Sydney S. Breise Jr.)

Will, L. 1914 Kolloidale Substanz als Energiequelle für die mikroskopischen Schusswaffen der Coelenteraten. *Abh. preuss. Akad. Wiss. Phys.-math. Kl.*, Nr. **1**, 1.

Appendix

To determine the angle between the axis of a pleated cylinder and the axis of the same cylinder when unfolded.

It is convenient to treat the two cylinders as flattened sheets, pleated or unpleated respectively, and to calculate the effect of a single pleat in a transverse edge on the tilt of this edge (figure 14).

In ΔRTR_1, let TR_1 be v and RT be x.

Then

$$v = \sin 90° - \theta' 2p,$$

$$x = \cos 90° - \theta' 2p.$$

In $\Delta R_1 Tr$,

$$\tan\alpha = \frac{v}{c-x} = \frac{\sin 90° - \theta' 2p}{c - \cos 90° - \theta' 2p},$$

$$= \frac{\sin 90° - \theta'}{c/2p - \cos 90° - \theta'} = \frac{\cos\theta'}{c/2p - \sin\theta'}.$$

With n pleats:

$$\tan\alpha = \frac{2np\cos\theta'}{c - 2np\sin\theta'} \quad \text{or} \quad \frac{\cos\theta'}{c/2np - \sin\theta'}.$$

This result is discussed on p. 152.

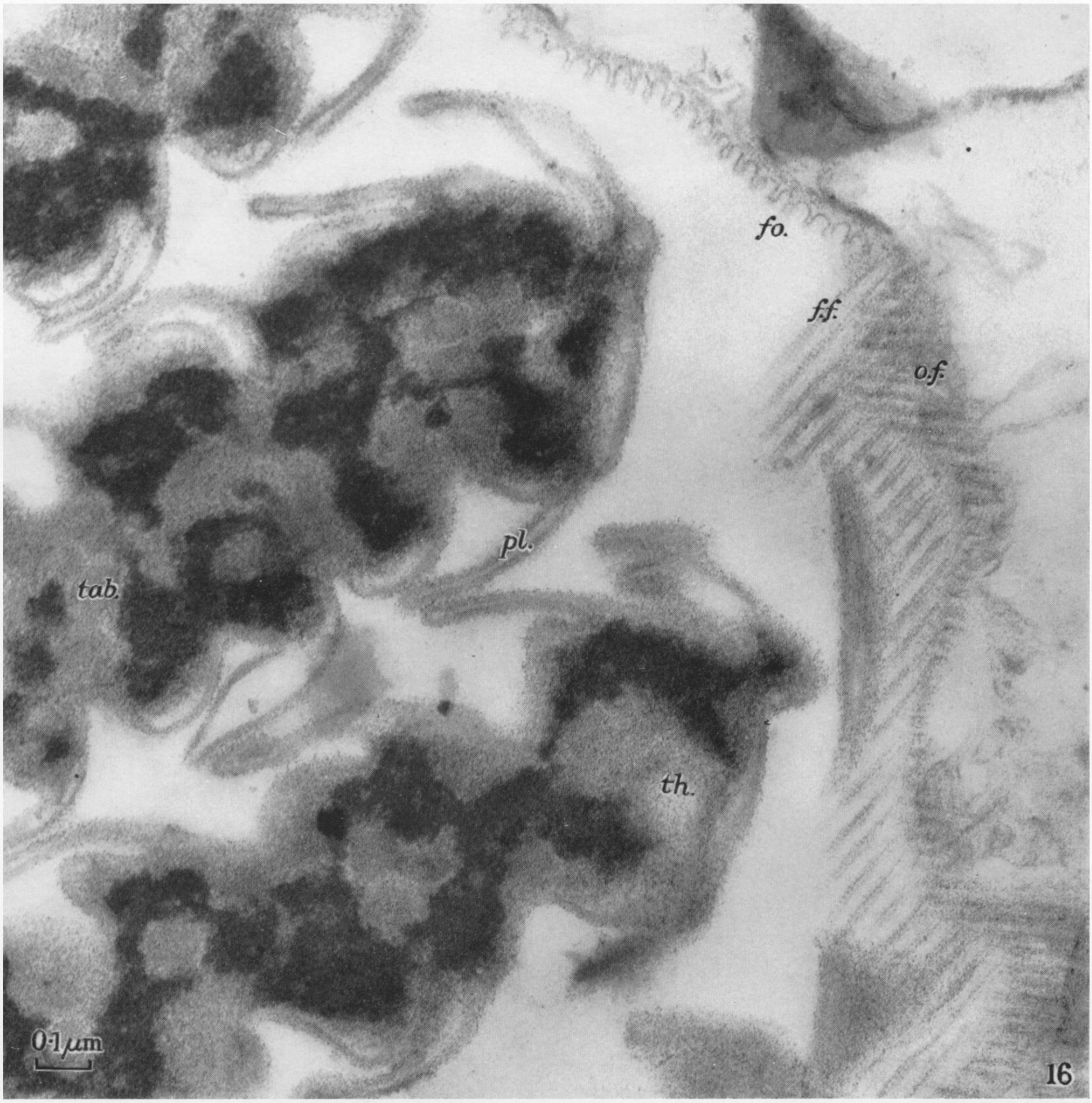

FIGURE 16. Tangential section of spirocyst capsule showing striated, outer fibres (*o.f.*); folds, *ca.* 350 Å thick (*fo.*), and finer fibrils (*ca.* 40 Å) (*f.f.*); longitudinal sections of the thread (*th.*); lightly and darkly stained thread contents, tabular crystal-like aggregates (*tab.*) and pleats (*pl.*).

FIGURE 17. Cross-section of capsule of a holotrichous isorhiza showing fine striation. Arrows mark discontinuities; crosses mark oblique, darker lines. Capsular fluid (*c.f.*); cnidoblast cytoplasm (*cyt.*).

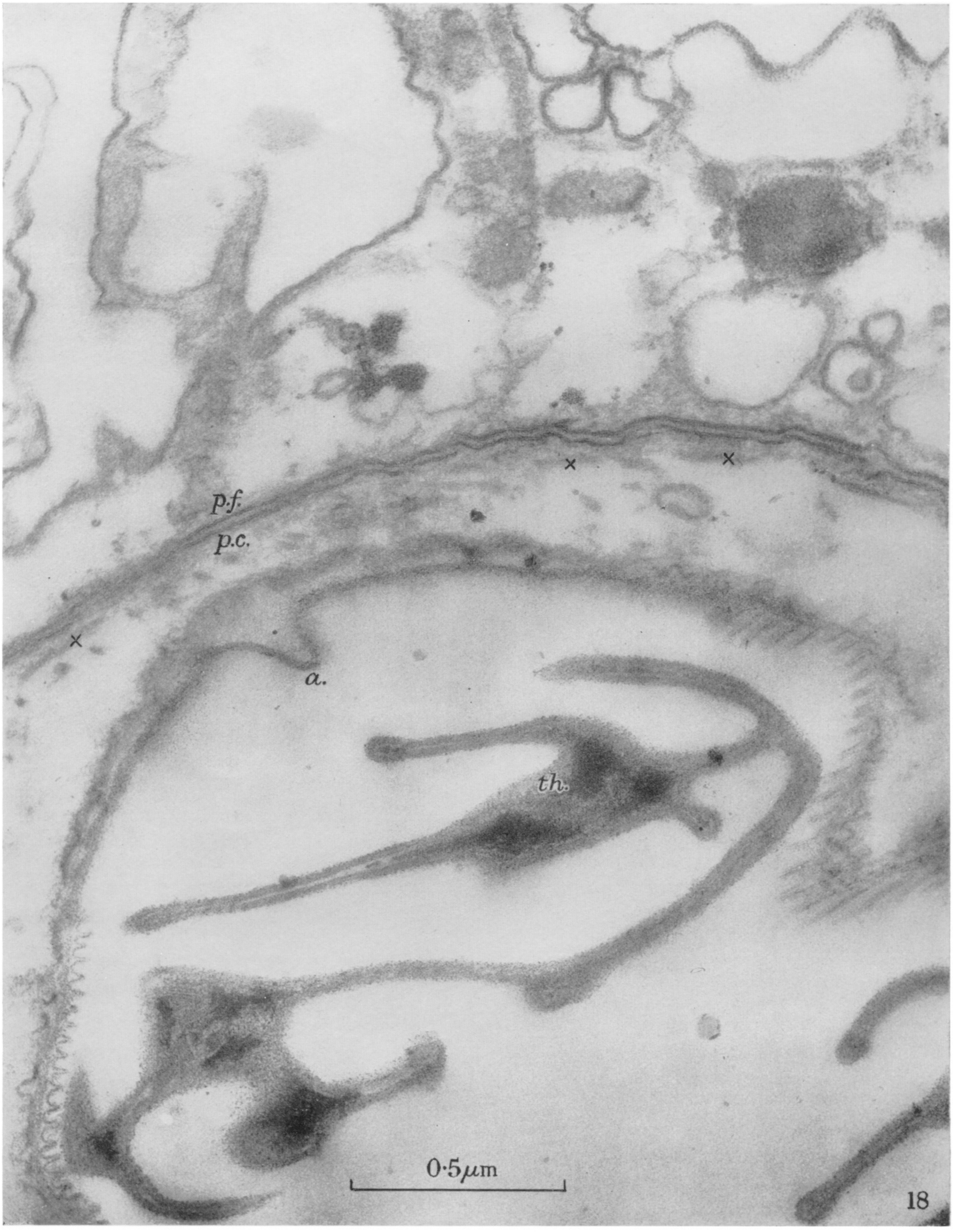

FIGURE 18. Longitudinal section of the distal end of a spirocyst showing change in structure of the capsule around the region of attachment (*a.*) of the thread (*th.*). Plasma membrane of cnidoblast (*p.c.*); plasma membrane of flagellated ectodermal cell (*p.f.*). The segments of cytoplasmic fibrils at × are characteristic of the cytoplasm covering the distal end of this type of capsule.

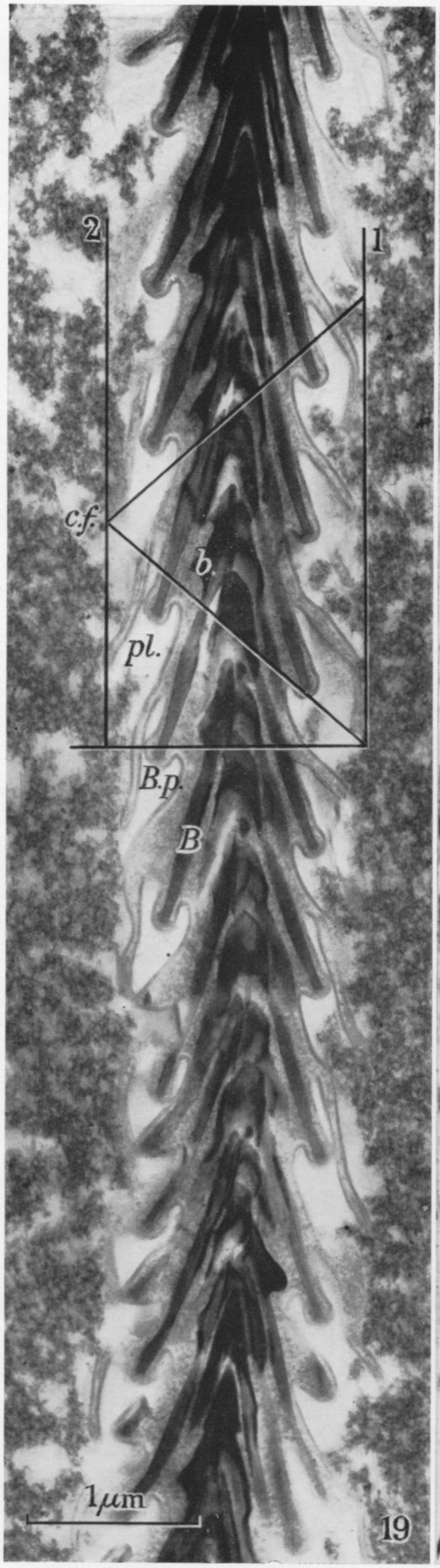

FIGURE 19. Median longitudinal section of the undischarged thread of a small holotrichous isorhiza, fixed in the capsular fluid (*c.f.*). (See text, p. 135.) Barb (*B.*), barb-pocket (*B.p.*), barbule (*b.*), pleats (*pl.*).

FIGURE 20. Transverse sections of the undischarged thread of a large holotrichous isorhiza fixed in the capsular fluid (*c.f.*).

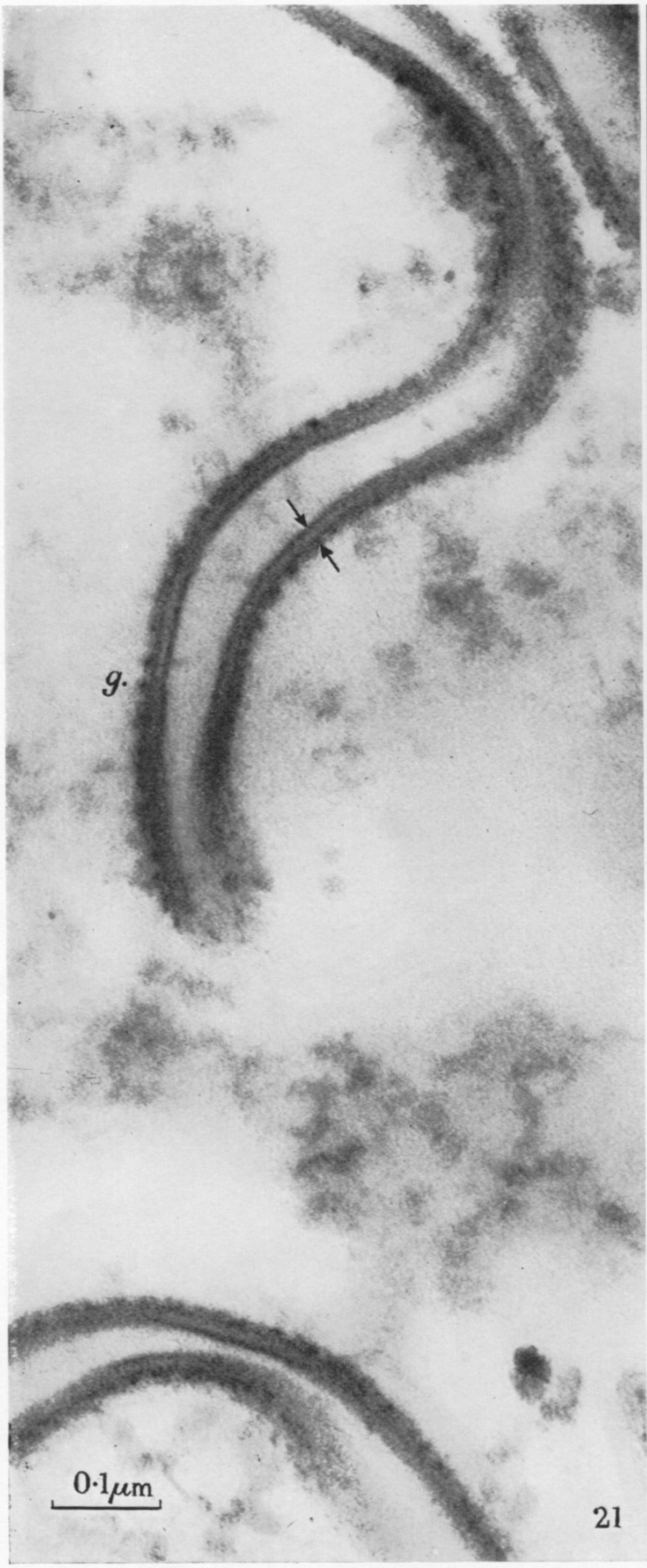

21

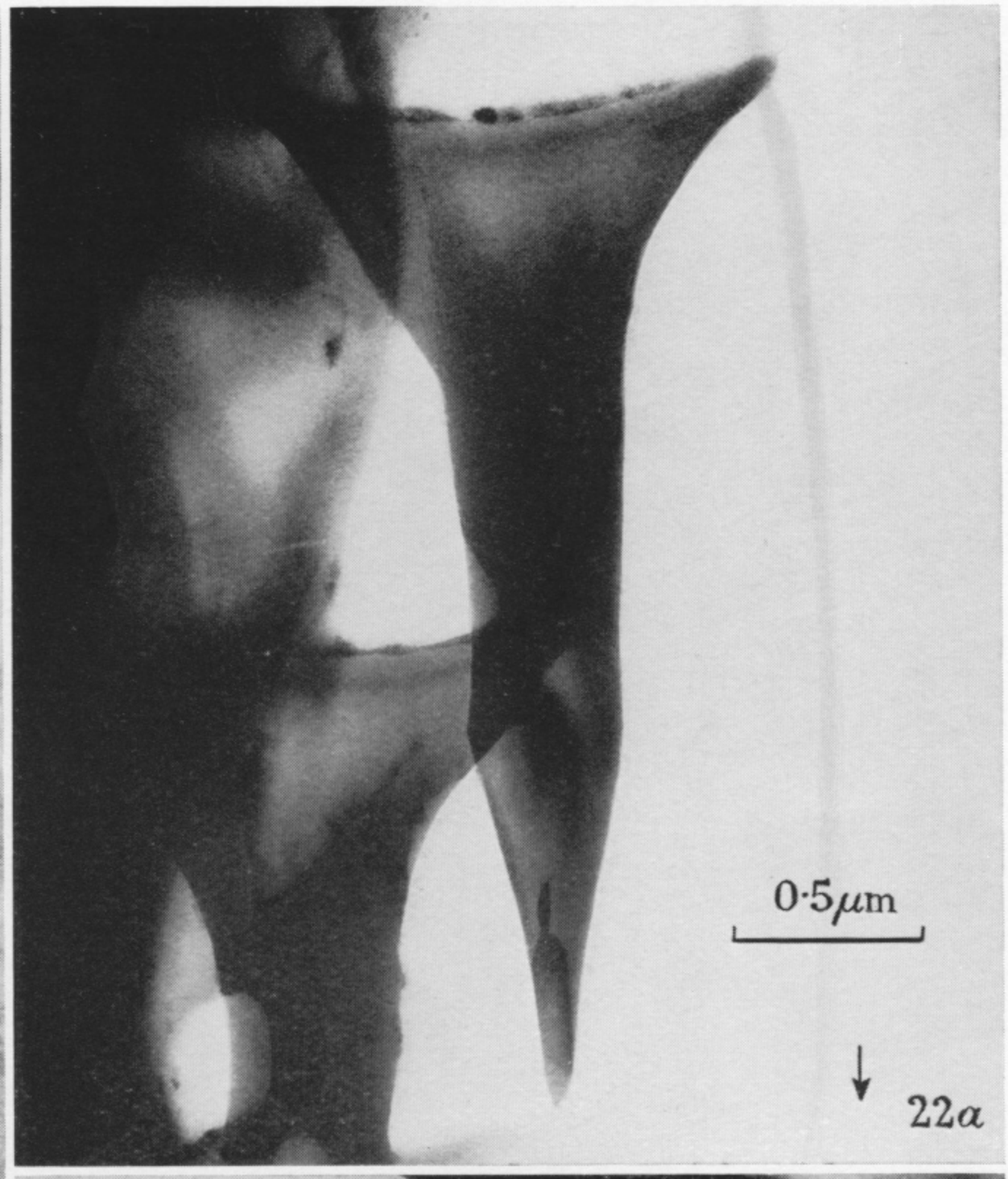

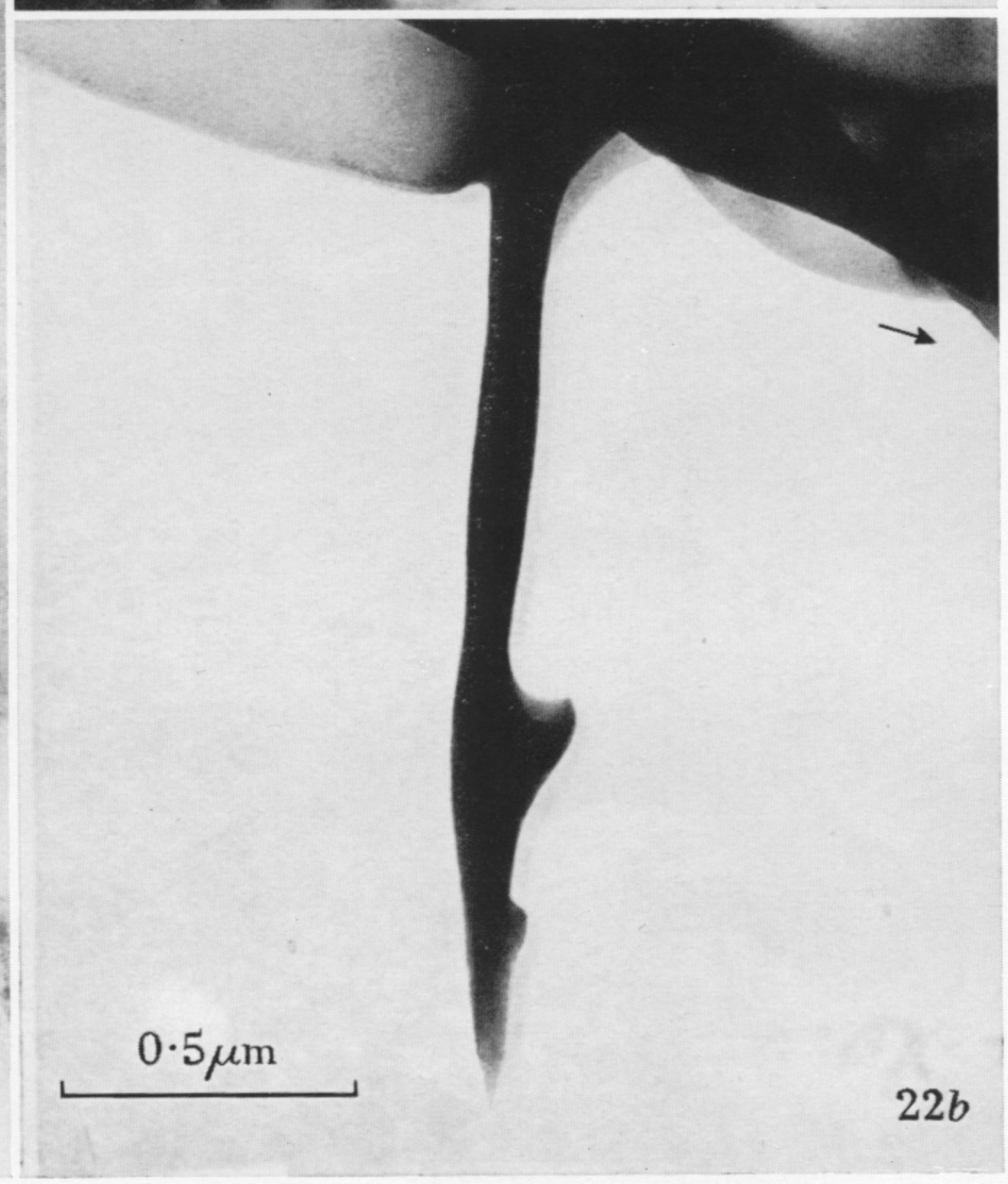

FIGURE 21. Transverse section of the wall of the undischarged thread of a large holotrichous isorhiza fixed in osmic-sucrose/sea water. The profiles of the wall are 160 Å thick (between arrows), finely striated, and bordered on each side by a dark line, in places apparently resolved into a row of granules. The surface in contact with the capsular fluid is covered by a layer of granules (*g.*), approximately 80 Å in diameter, in open array.

FIGURE 22. Single barbs on the discharged thread of a large holotrichous isorhiza, dried in air; (*a*) in plan; (*b*) in side view. The arrows point towards the capsule.

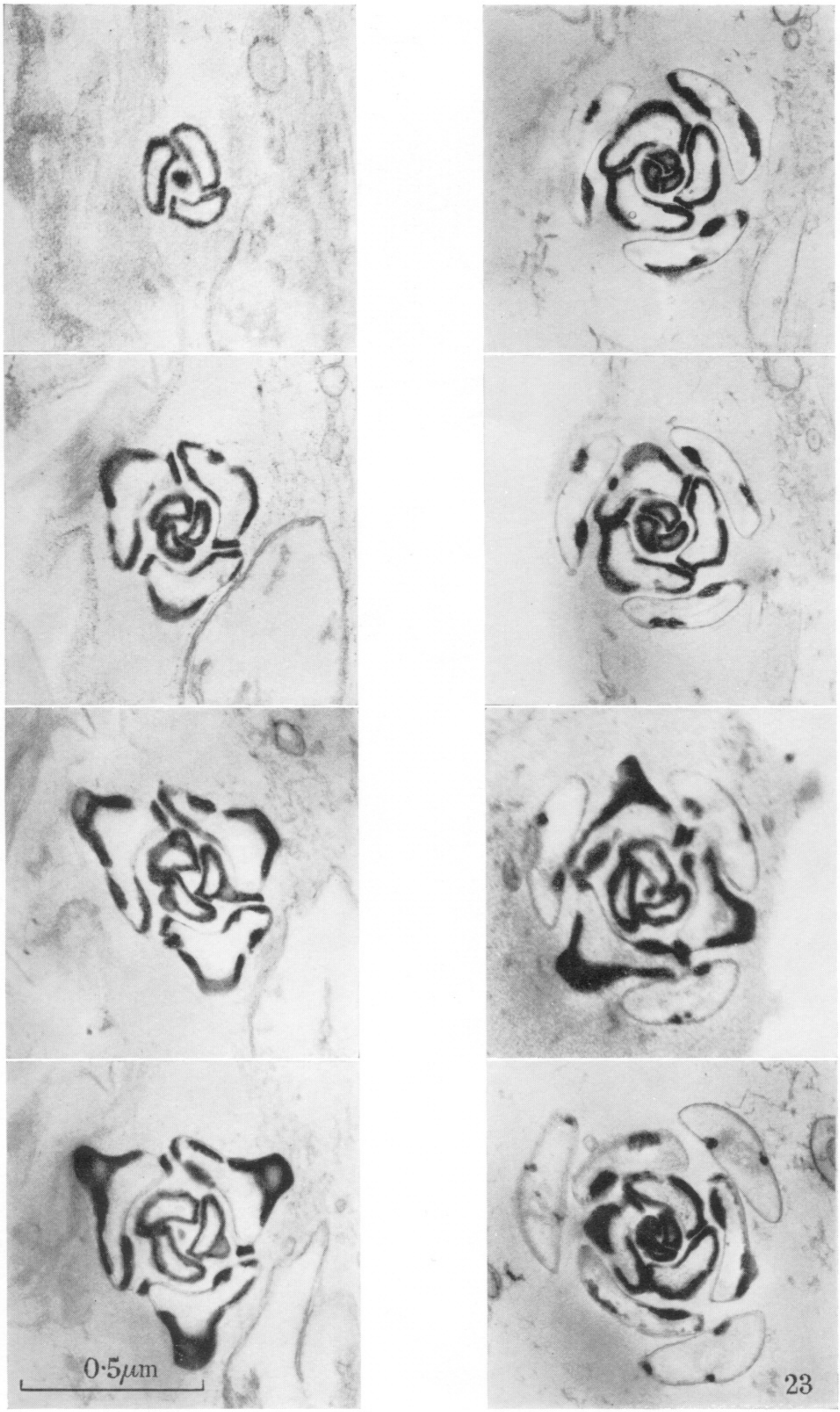

FIGURE 23. Accurately transverse serial sections of a dart from a thread arrested in discharge in a smear from a tentacle, showing the overlap between barbs of the same whorl, and the high electron-density of the barbules and of asymmetrically placed regions of the shaft.

FIGURE 24. Longitudinal section of an undischarged capsule of a microbasic mastigophore. The barbs (*B.*) (see text, p. 138) are strongly curved and without barbules.

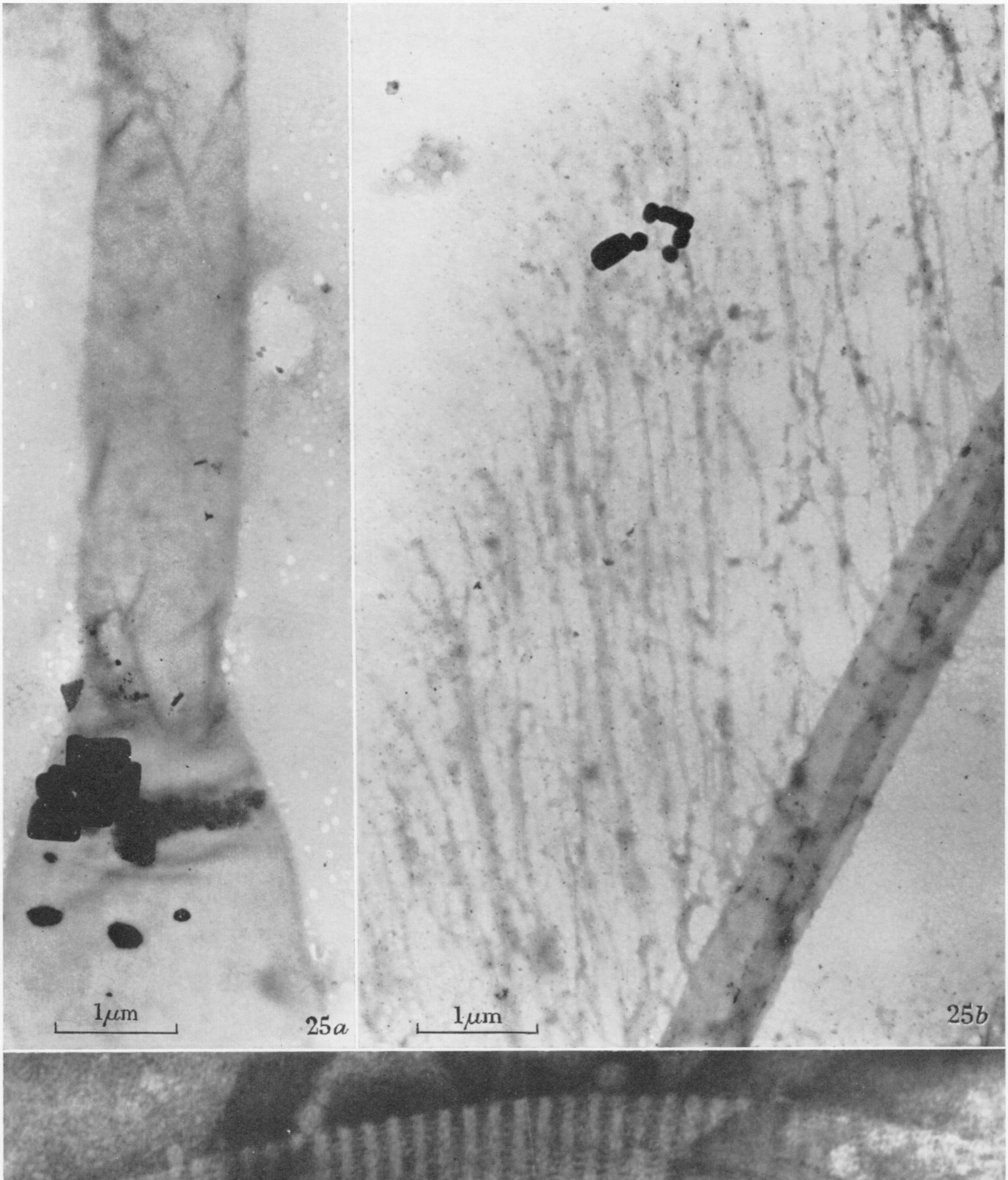

FIGURE 25. (*a*) Discharged spirocyst-capsule (air dried) showing faint helical markings of steep inclination on the lower part of the discharged thread. (*b*) The *Flimmer*-like anastomizing strands of material on one side of the discharged thread. The 'core' of the thread is probably a fold in the thin tubular wall, and the dense particles may be sodium chloride.

FIGURE 26. Scar marking the attachment of a barb to the surface of the discharged thread of a large holotrichous isorhiza, air-dried and negatively stained with potassium phosphotungstate.

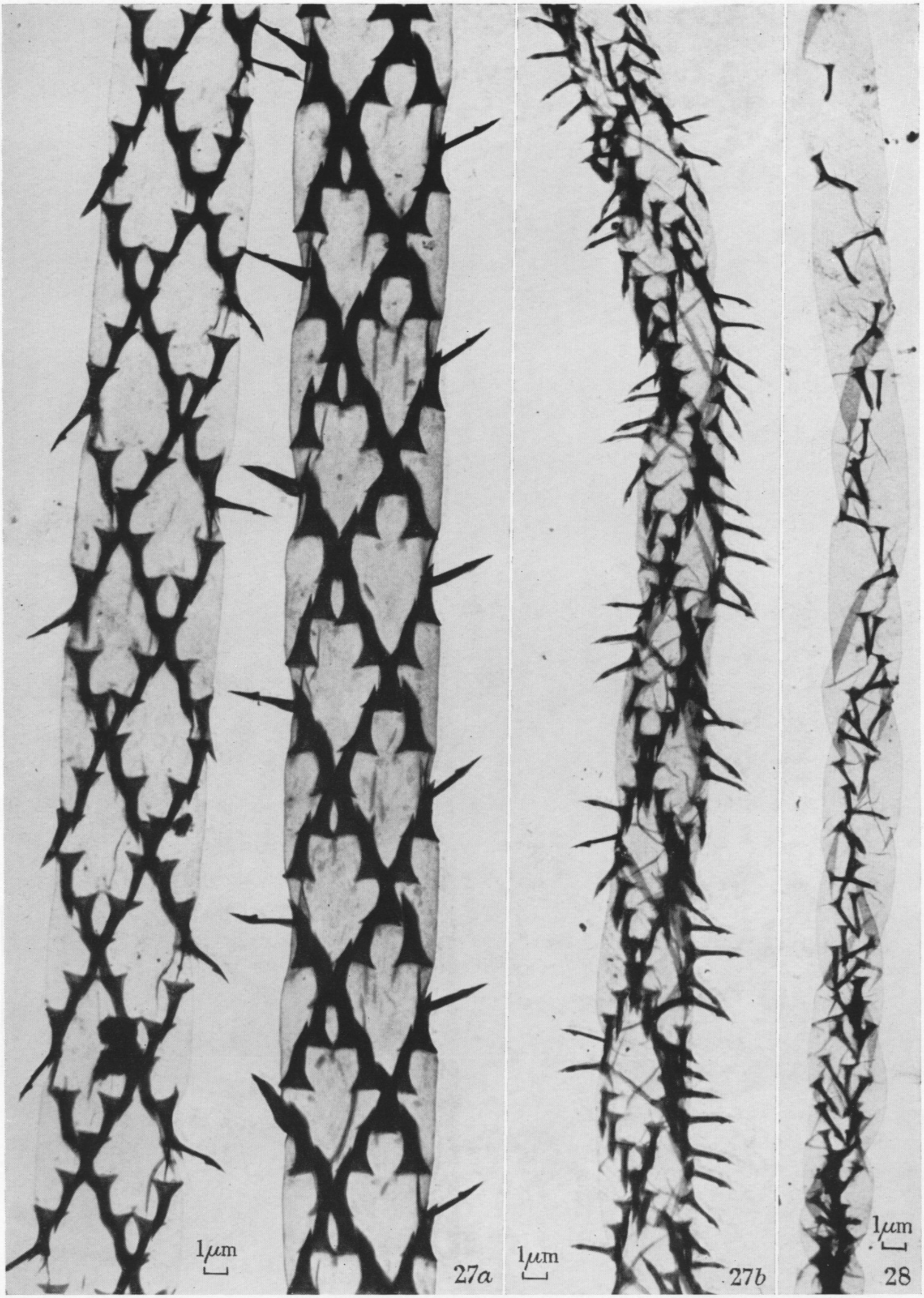

FIGURE 27. Air-dried discharged threads from two holotrichous isorhizas (*a* and *b*), flattened to differing extents, showing barb-whorls and the staggering of the whorls, so as to form three rows of barbs.

FIGURE 28. Air-dried thread discharged without eversion by bursting the capsule of a holotrichous isorhiza in distilled water. The most anterior barb, without near neighbours, is as asymmetrical as those in triads. The tip of the thread is just off the top of the photograph.

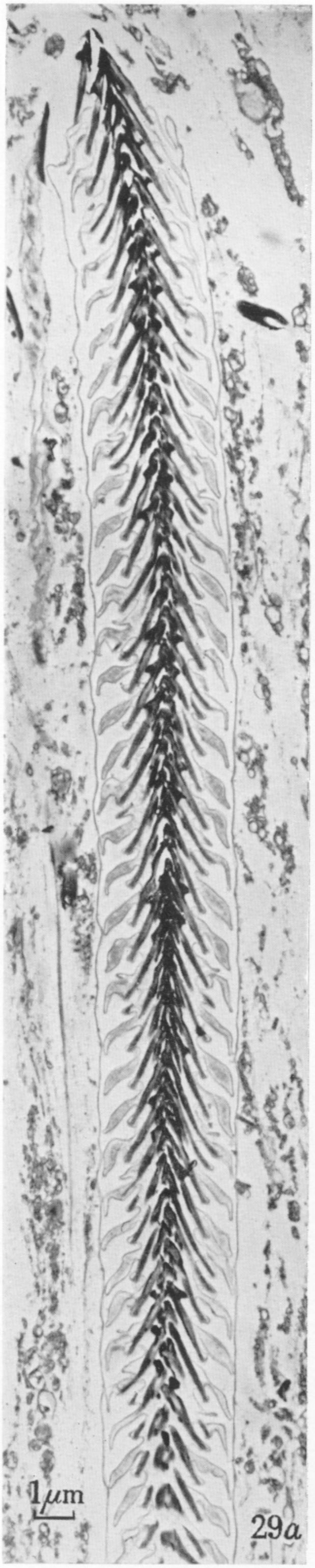

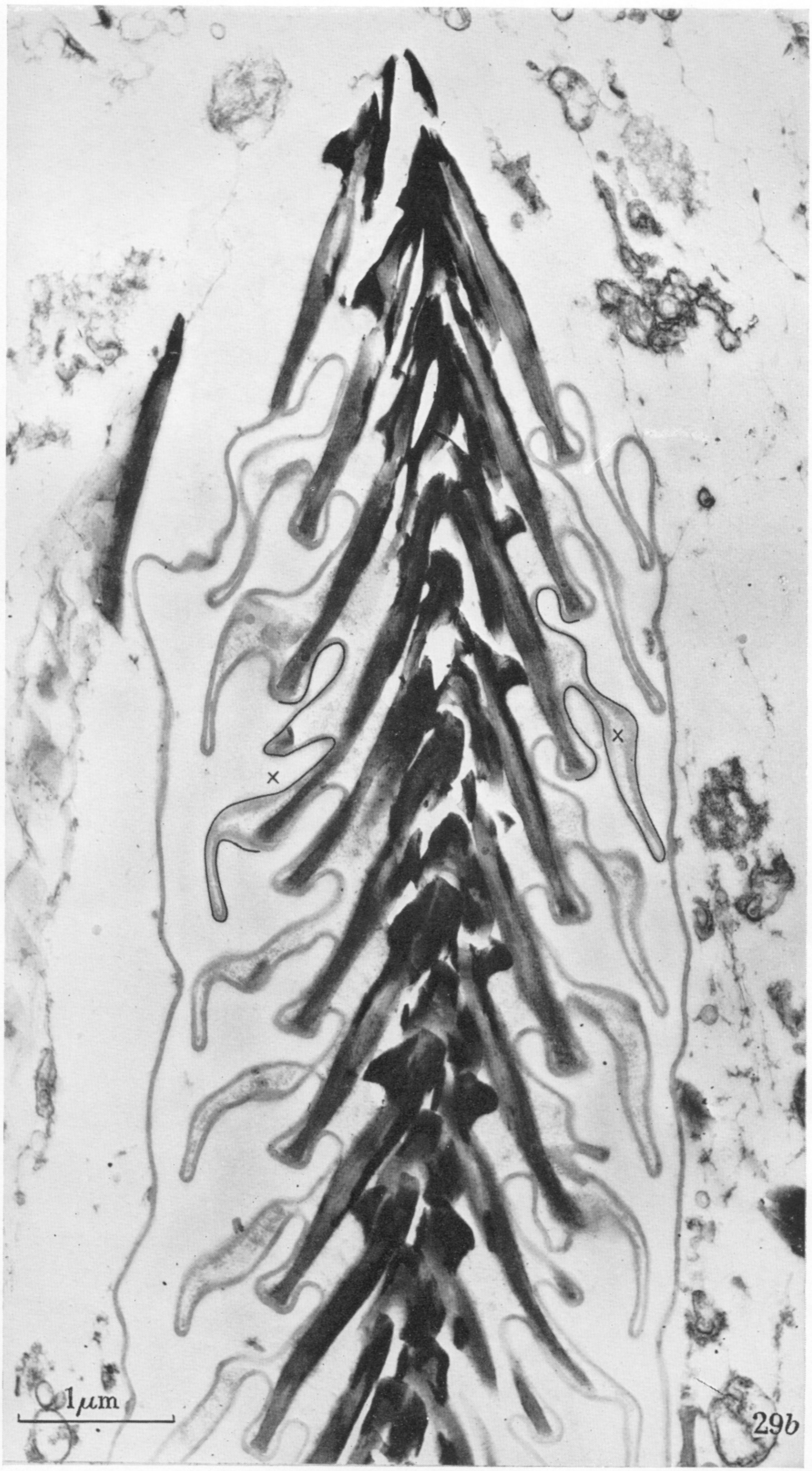

FIGURE 29. (*a*) Accurately median longitudinal section of dart and thread of a large holotrichous isorhiza arrested in discharge in a tentacular smear. (*b*) The dart and tip of this same section under higher power. The barbs have fallen from the discharged surface. In *b* the inked-in right- and left-hand profiles are those used to determine the area of the internode (p. 149). In each case the cross marks the centroid of the curve.

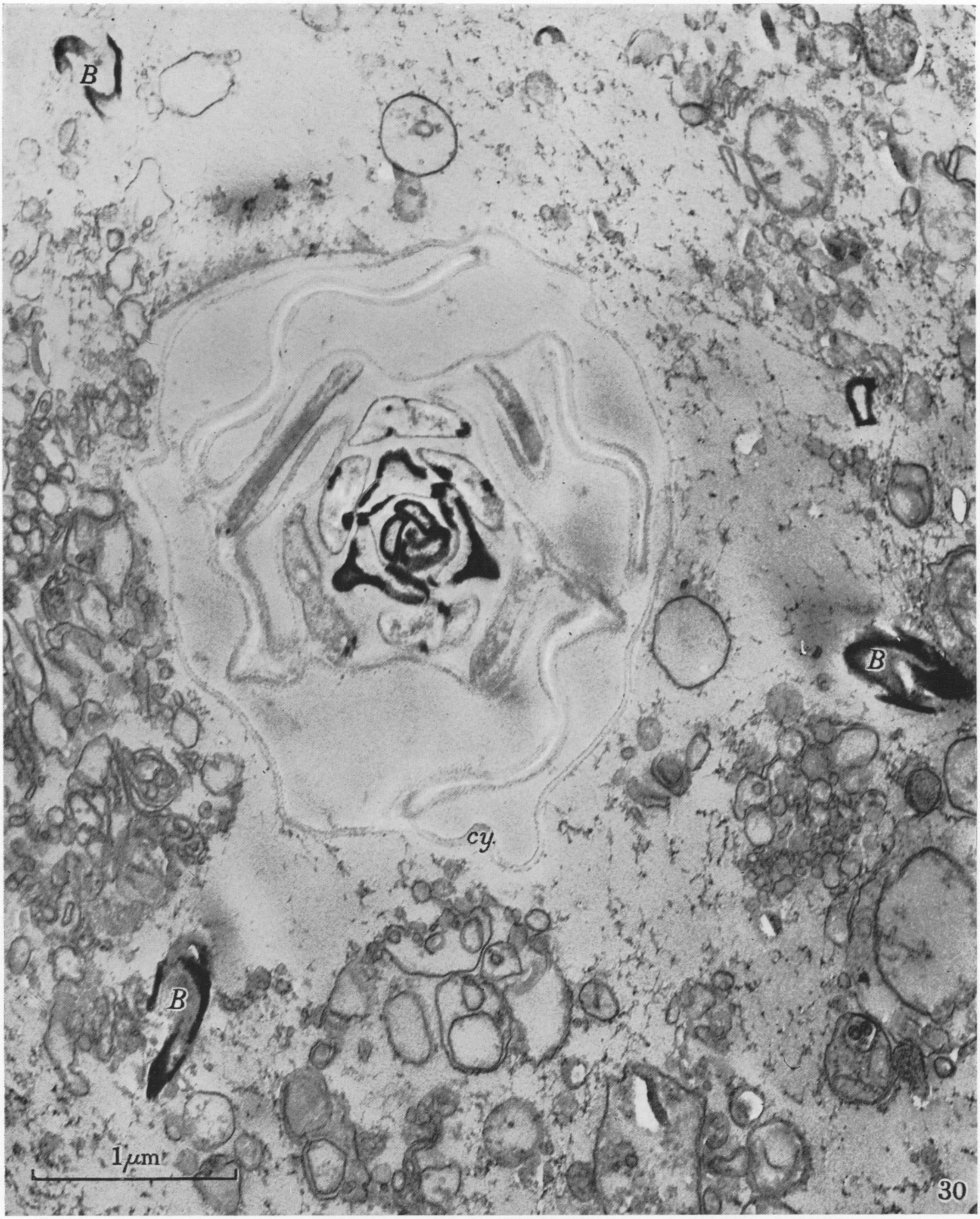

FIGURE 30. Accurately transverse section of an arrested tip, showing portions of one whorl of barbs (*B.*) from the outer surface of the discharged cylinder itself (*cy.*) and th eundischarged thread (as in figure 20, plate 14) within.